RMP
REGIONAL MONITORING
PROGRAM FOR WATER QUALITY
IN SAN FRANCISCO BAY

sfei.org/rmp

San Francisco Bay
Interim Model Validation Report

Prepared by

Rusty Holleman, SFEI

Emma Nuss, SFEI

David Senn, SFEI

CONTRIBUTION NO. 850 / DECEMBER 2017

SAN FRANCISCO ESTUARY INSTITUTE • CLEAN WATER PROGRAM/RMP • 4911 CENTRAL AVE., RICHMOND, CA • WWW.SFEI.ORG

San Francisco Bay

Interim Model Validation Report

Rusty Holleman

Emma Nuss

David Senn

December 2017

SFEI Contribution #850

This work was funded as a result of settlement of San Francisco Bay Water Board enforcement actions and by the Nutrient Management Strategy

Table of Contents

1 Summary

As part of the Nutrient Management Strategy, a coupled hydrodynamic-biogeochemical model of San Francisco Bay is being developed. The process-based, numerical model will be used to inform nutrient management decisions, by:

- improving quantitative understanding of processes that shape current conditions,
- forecasting ecosystem response under future scenarios, and
- evaluating potential effectiveness of management actions.

This report describes the model in its present configuration and the status of its validation. Model development is necessarily an iterative process, with early stages focused on refining the model's representation of hydrodynamics and transport, and later stages of the effort including increasingly complex representations of biogeochemistry. Present validation efforts focus on assessing model skill with respect to hydrodynamics, salinity and transport. The final report will additionally consider model validation of water quality and biogeochemical processes.

The model inputs include tides, direct precipitation, evaporation, stormwater runoff, wastewater discharges, Delta outflow and wind. From these inputs, the model calculates water levels, salinity, currents and the force of the currents on the bed throughout the Bay. Simulations cover the period October 2012 through September 2013 (water year 2013).

A wide range of observations collected throughout the Bay are used to assess the model's predictive skill. Comparisons between observed and modeled data include tidal water levels, depth-averaged velocities and salinity from both shipboard and moored sensors.

Water levels are reproduced well from South Bay up to San Pablo Bay. Tidal comparisons upstream of Carquinez Strait show that the model generally overpredicts water levels, likely due to the truncated upstream Delta. Velocities are modeled similarly well in open areas of the Bay downstream of Carquinez Strait. Velocities upstream of Carquinez Strait likewise belie the lack of a resolved Delta.

Salinity is compared to monthly USGS transects along the channels of the Bay. Overall skill in predicting salinity is good, with a small bias fresh in the summer likely due to the absence of evaporation. Comparisons to transect data are augmented by moored, time-series data at three sites. These comparisons show that in the dry season the model exhibits a bias towards being too fresh, but wet season events are captured very well.

The hydrodynamic model in its current state has sufficient skill in representing transport in South Bay to support water quality studies with a South Bay focus. Velocities and water levels upstream of San Pablo Bay suffer from proximity to the Delta boundary condition. This may lead to unrealistic transport in Suisun Bay, and has been part of the motivation for Suisun and Delta-specific modeling efforts which include the Delta. Further work is needed to achieve similar fidelity for exchange with the coastal ocean and transport in North Bay.

The remainder of this report provides details on the configuration of the model, analysis of its skill, and discussion of potential causes for model–data disagreements.

2 Model Setup

The San Francisco Bay hydrodynamic model is built on *D-Flow Flexible Mesh* (DFM). DFM is part of the Deltares suite of models which also includes *D-Water Quality*, the platform chosen for the biogeochemical phase of the NMS modeling project. DFM is a finite-volume, three-dimensional, unstructured hydrodynamic model (Martyr-Koller *et al*, 2017). The unstructured nature of the grid allows for efficient and flexible resolution of flow features ranging from small perimeter sloughs and ponds up to a regional representation of the coastal ocean. This range of features is resolved without explicit seams or nesting boundaries as would be required for a structured grid model applied to the same area.

The original model setup was developed by Silvia Pubben and Mick van der Wegen, (Pubben, 2017), as a continuation of prior modeling efforts stemming from the USGS CASCaDE and San Francisco Bay-Delta Community Model projects.

We set up the model to simulate Water Year 2013 (WY2013), which spans October 30, 2012 to September 30th, 2013. The simulation begins two months earlier on August 1, 2012 to allow the model to spin up.

WY2013 was chosen based on overlap with important recent data collection efforts (i.e. ADCP deployments), and the desire to avoid the more anomalous drought conditions of later years.

The model has been run on a Linux workstation utilizing 16 Intel Xeon E5-2680 2.40 GHz cores, communicating over MPI. The full 426 day run takes 7.0 days of wall-clock time, for a simulation speed of 61 times faster than realtime. DFM was compiled from SVN revision 52184 of the source code and GCC 5.4.0.

3 Model Domain and Grid

The model domain covers San Francisco Bay, including portions of Coyote Creek and Guadalupe River at the southernmost extent of the Bay, and extending north to the Sacramento and San Joaquin Rivers at Rio Vista and Jersey Point, respectively. A separate but related model includes a complete Delta, however the computational expense of that model currently limits its utility to studies with a North Bay focus, while the present model is optimized for South Bay applications. The domain extends into the Pacific Ocean, about 20km west of Point Reyes in the north and 40km west of Half Moon Bay in the south, roughly encompassing the San Francisco Bight. The horizontal grid resolution varies from 20 m in select sloughs of Lower South Bay, to over 2 km at Point Reyes. Nominal grid resolution in South Bay is 250 m, and 350–500 m in North Bay, for a total of 49,996 cells in the horizontal. The three-dimensional model utilizes a sigma coordinate in the vertical, such that all areas have 10 layers in the vertical, with the layer thicknesses varying in accordance with the overall depth.

Bathymetry for the model has been compiled from a combination of digital elevation models (DEMs):

- 10 m topo-bathymetry[1] from California Department of Water Resources (Wang and Ateljevich, 2012).
- High resolution USGS bathymetry[2] in Lower South Bay (Foxgrover et al, 2014).

Bathymetry is prescribed at the nodes of the grid by linear interpolation on the source DEMs, then internally extrapolated to edges and cells. All elevation data are relative to the NAVD88 vertical datum.

[1] http://baydeltaoffice.water.ca.gov/modeling/deltamodeling/modelingdata/DEM.cfm
[2] https://pubs.usgs.gov/of/2011/1315/

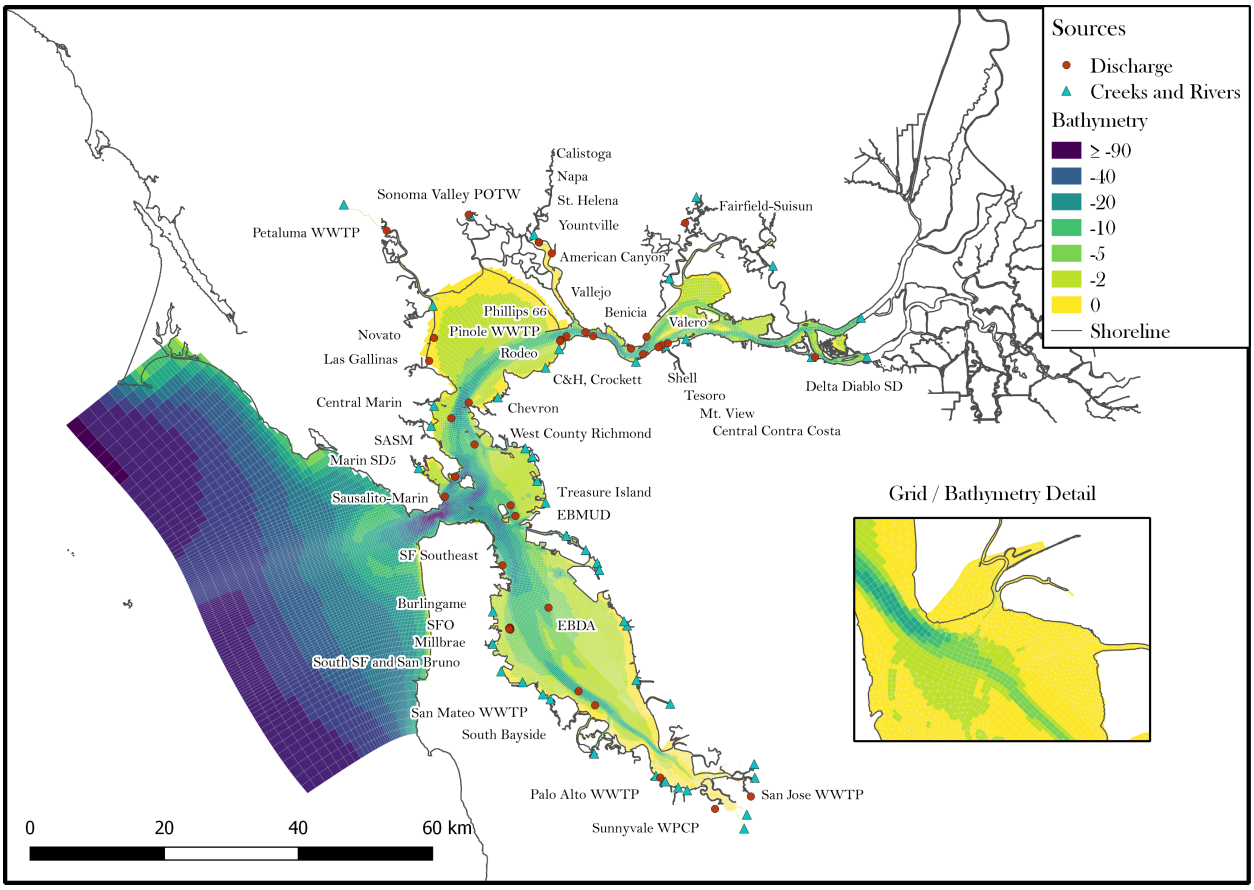

Figure 1: San Francisco Bay DFM grid

4 Boundary Conditions and Forcings

4.1 Tidal Ocean Boundary

The open ocean boundary is forced along the western edge by observed sea level data from Point Reyes, via NOAA gage 9415020. Observed 6-minute water levels are low-pass filtered with a 4th order Butterworth filter with a 3-hour cutoff period. Salinity at the ocean boundary is set to a constant 33 ppt. The shorter northern and southern edges of the ocean boundary are closed.

4.2 Bay Area Rivers and Stormwater

Freshwater flows were derived from the *Bay Area Hydrologic Model* (BAHM), an HSPF-based hydrologic model. This model has been calibrated against gage data over the 2000–2016 period, and includes 44 separate

river and stormwater inputs to the Bay. All river and stormwater inputs are assumed to enter the Bay with negligible salinity.

4.3 Delta Inflow

To avoid undue computational complexity the hydrodynamic model does not extend into the Sacramento–San Joaquin Delta. The edge of the model domain is at Rio Vista on the Sacramento River and Jersey Point on the San Joaquin River, well within the tidal portion of the system. Boundary conditions here are taken from USGS streamflow gages, specifically USGS stations 11455420 (Sacramento River at Rio Vista) and 11337190 (San Joaquin River at Jersey Point) for the Sacramento and San Joaquin flows, respectively. Flows at Rio Vista and Jersey Point are assumed to have negligible salinity.

4.4 Wastewater Treatment Plants and Refineries

Given the goal to support nutrient-related studies in the Bay, special attention has been given to Wastewater Treatment Plant (WWTP) inputs. In parts of the Bay, especially South Bay, WWTP inputs are significant freshwater sources and it is therefore essential that they are accounted for in the hydrodynamics where they can properly influence the density field (as opposed to added as mass sources in the water quality model). Flow and load data for 37 WWTPs and 5 refineries have been compiled and made available online via ERDDAP[3] and github[4]. This compilation draws on observed flow rates where data exist. For dates when flow data is unavailable, a flow rate is estimated based on inter-annual trends and a seasonal flow climatology. Each of the 42 inflows have been added to the hydrodynamic model as a freshwater source located at the bed.

4.5 Winds

The model includes a wind field derived from observations at 5–10 stations near the Bay (depending on data availability). These observations have been extrapolated in space based on the method of Ludwig *et al* (1991), which uses topographic data, atmospheric stability and observed winds to extrapolate a smooth,

[3] http://sfbaynutrients.sfei.org/erddap/tabledap/sfei_sfbay_potw_201705.html
[4] https://github.com/rustychris/sfbay_potw

terrain-aware wind field. The hydrodynamic model includes the effects of wind in terms of surface stress and vertical mixing, but does not yet include wind-waves.

4.6 Precipitation and Evaporation

In addition to stormwater runoff which enters the model at prescribed locations along the boundary, we also include direct precipitation and evaporation acting directly on the water surface. The model incorporates measured precipitation and evapotranspiration ($ET_\circ$) from the CIMIS Union City station. $ET_\circ$ is scaled to pan evaporation[5] by dividing by a factor between 0.6 and 0.7 depending on temperature. The present model configuration further scales this evaporation down by a factor of 2 due to transient stability issues, though this factor will be removed in the near future as those stability problems are resolved. These inputs have the greatest effect in South Bay due to long residence times and minimal local freshwater inflows. Given these conditions, using a South Bay data source across the entire domain has not been problematic.

5 Validation

Accurately predicting tidal water levels and velocities is fundamental and essential in a system like San Francisco Bay in which tides are the dominant driver of transport and mixing. Given the water quality applications of this model, skill in predicting salinity is perhaps even more important because the salinity field integrates the combined effects of sources, transport and mixing, both in the model and in nature. In this sense, a good validation for salinity is a much stronger indicator than water level or velocity that nutrients and plankton will also be transported correctly. Salinity is also important due to its role as an active driver of flows, where salinity gradients equate to density gradients which in turn drive circulation in marine environments.

The hydrodynamic model is validated against observations of tidal water level, velocity and salinity. Data from NOAA tide gages around the Bay are compared to model outputs for validation of tidal phase and amplitude. Validation of the velocity field draws on a series of short-term Acoustic Doppler Current Profiler (ADCP) moorings deployed by NOAA in 2012–2013. The modeled salinity field is compared to data from USGS cruises along the thalweg of the Bay. The cruises collect vertical profiles of salinity and other

[5] https://cals.arizona.edu/azmet/et1.htm

constituents at 36 stations, allowing for validation of both the longitudinal salinity field and salt stratification. Several USGS moored salinity sensors are also included which provide a more complete comparison of salinity variation at time scales from hours to weeks.

While in some systems temperature has an effect on transport similar to salinity, density variation in San Francisco Bay is dominated by salinity, leaving temperature with a negligible role. For this reason, temperature is not part of the present model or its validation. For the purpose of water quality modeling, in which process rates can be strongly temperature-dependent, we synthesize a spatially and temporally varying temperature field from observational data. A related modeling effort carried out by Deltares collaborators has included a mechanistic temperature model (Vroom et al., 2017), which may be incorporated into this model in the future.

5.1 Definition of Metrics

In addition to graphical figures comparing modeled and observed quantities, we present several numeric measures of predictive skill, defined below. In these definitions a horizontal line ($\bar{x}$) indicates the arithmetic mean, and a subscript x_i indicates individual samples of the respective dataset.

Skill Model skill is calculated according to the formula proposed by Willmott, 1981,

$$SS = 1 - \frac{\sum_i (m_i - o_i)^2}{\sum_i \left(|m_i - \bar{o}| + |o_i - \bar{o}|\right)^2},$$

where o_i denotes samples in the observed data, m_i denotes samples in the model results. A perfect model achieves a skill score of 1. Unlike the correlation coefficient, the skill score takes into account both the correlation and the relative scales of the modeled and observed data.

Bias The average error, $\overline{m_i - o_i}$.

r^2 The squared correlation coefficient, defined as

$$r^2 \equiv \frac{C_{mo}^2}{C_{mm} C_{oo}},$$

where C_{ij} is the covariance matrix computed between the model and observed data. A value of 1.0

indicates perfect correlation or anti-correlation, and a value of 0.0 indicates no correlation between the model and observed data.

RMSE Root mean squared error, $\left(\overline{(m_i - o_i)^2}\right)^{\frac{1}{2}}$.

Lag The time shift, in minutes, between the model time series and the observed time series. A positive values means that the model *lags* the observations, and a negative value means that the model *leads* the observations.

Amplification factor The ratio of standard deviations between the model and the observations. A factor of 1.0 is perfect, while a factor greater than 1 indicates that the signal is amplified in the model, and a factor less than 1 indicates that the signal is attenuated or under-represented.

Threshold values separating success from failure are often difficult to generalize for these metrics. Here we describe some baseline expectations for a successful validation, with the caveat that the details of whether the validation is sufficient is often site and application specific. Water level is the most fundamental, and typically the easiest, quantity to validate, and we expect to have skill and correlation coefficients well above 0.9. Time lags should be much shorter than the period of the tides. Velocity, and specifically velocity magnitude, exhibits much greater small-scale variability than water levels. For this reason, individual ADCP comparisons tend to have larger RMSE and somewhat greater lags than water level comparisons. Where an amplitude error of 10% would be problematic for water levels, this is more often acceptable for velocity comparisons. Skill metrics for salinity at the scale of this model require nuanced interpretation due to the wide range of processes which contribute to salinity distributions. Where possible we include descriptions of specific patterns of errors which can be related to a specific aspect of the model. For the limited number of salinity time series stations, we also present skill metrics.

5.2 Water Level

NOAA tide gages record six minute water level data at numerous sites around the perimeter of the Bay. Validation of water levels at tidal time scales is an essential baseline metric for a coastal hydrodynamic model. The most relevant metrics for tidal validation in open areas of the Bay are the amplitude and lag. Tides are amplified and attenuated due to geometry and frictional characteristics of the Bay, a process which is capture

by the comparison of amplitudes. The timing or phase of water level is driven by the same characteristics, with friction generally slowing the propagation of the tidal wave, and convergent or enclosed basin geometries causing an apparent acceleration of the tidal wave (a “standing wave”).

The model has been calibrated for tidal phase and amplitude at San Francisco by adjusting tidal conditions at Point Reyes before applying that water level as the ocean boundary condition. Performance within the Bay is quite good, with almost no additional amplification or attenuation aside from Port Chicago. Phase is also well represented at the open Bay sites, with phase leads less than 10 minutes. Phasing at Redwood City is complicated by local, dissipative features and the fact that the tide gage is sited in a perimeter slough. Phase and amplitude at Port Chicago indicate the limitations of the northern portion of the domain and the lack of a resolved Delta.

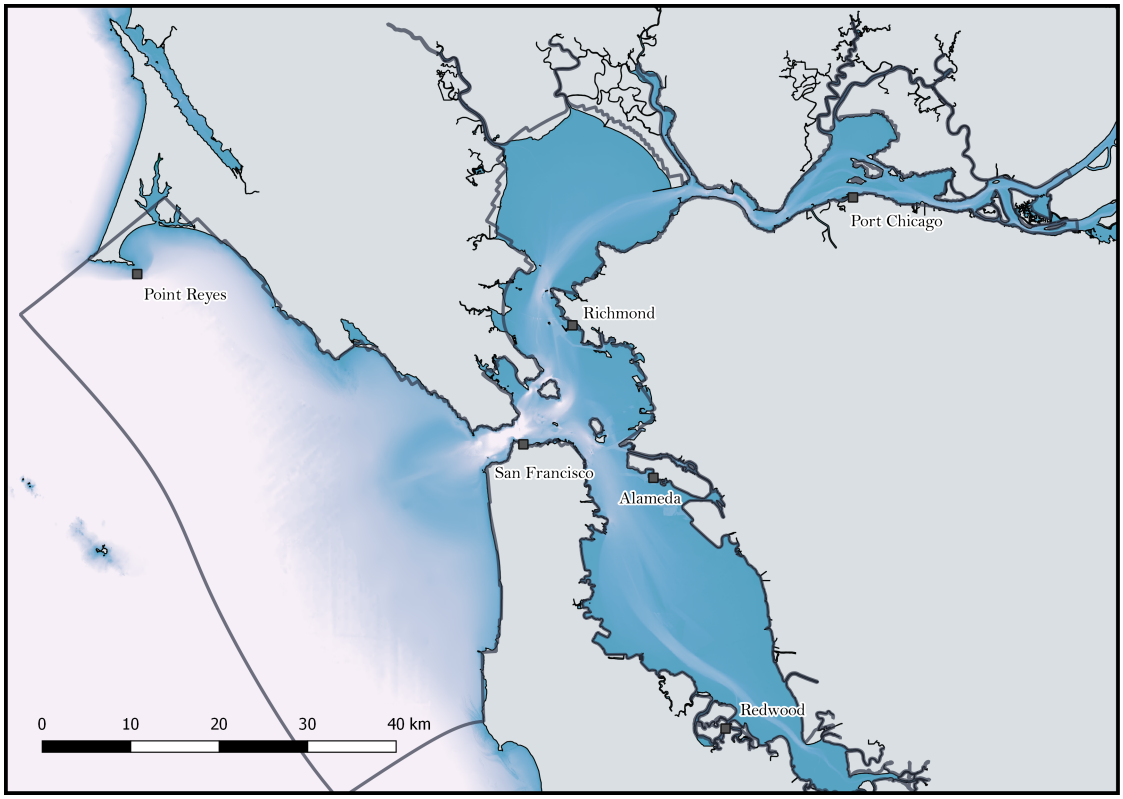

Figure 2: Locations of NOAA water level gaging stations

Name	Skill	Bias (m)	r^2	RMSE (m)	Lag (min)	Amp. factor
San Francisco	0.999	-0.010	0.996	0.035	0.1	1.00
Point Reyes	0.993	0.039	0.991	0.085	3.1	0.89
Richmond	0.998	–	0.992	0.055	-5.5	1.04
Alameda	0.997	0.024	0.991	0.068	-8.4	1.04
Redwood City	0.992	–	0.968	0.136	-19.7	1.02
Port Chicago	0.894	0.014	0.864	0.394	-37.7	1.72

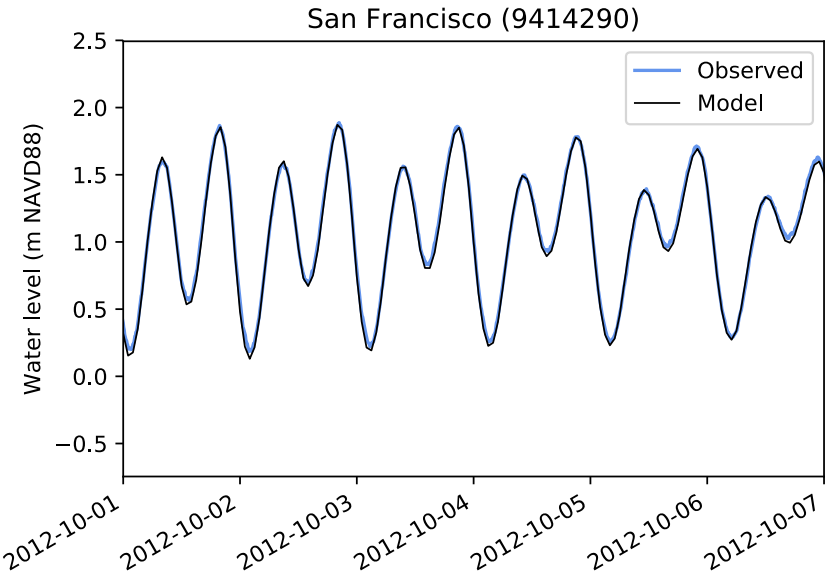

Figure 3: Water level comparison at San Francisco

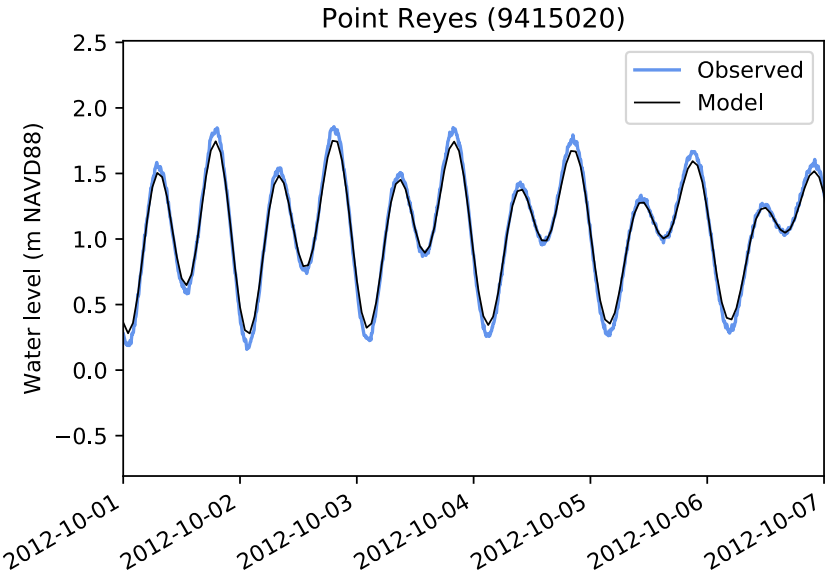

Figure 4: Water level comparison at Point Reyes

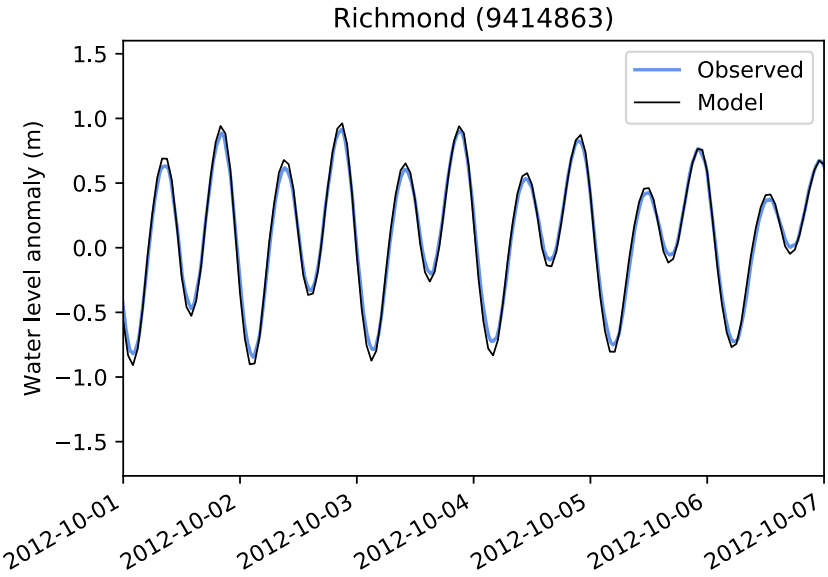

Figure 5: Water level comparison at Richmond

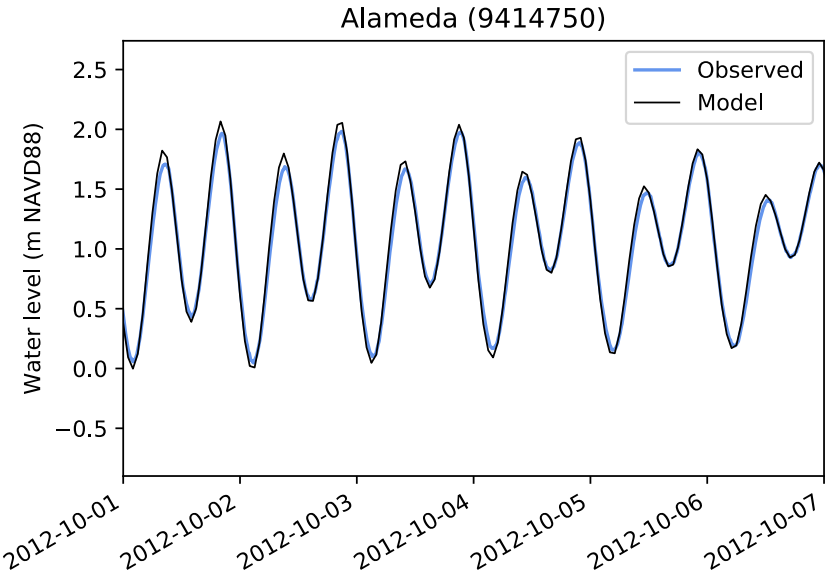

Figure 6: Water level comparison at Alameda

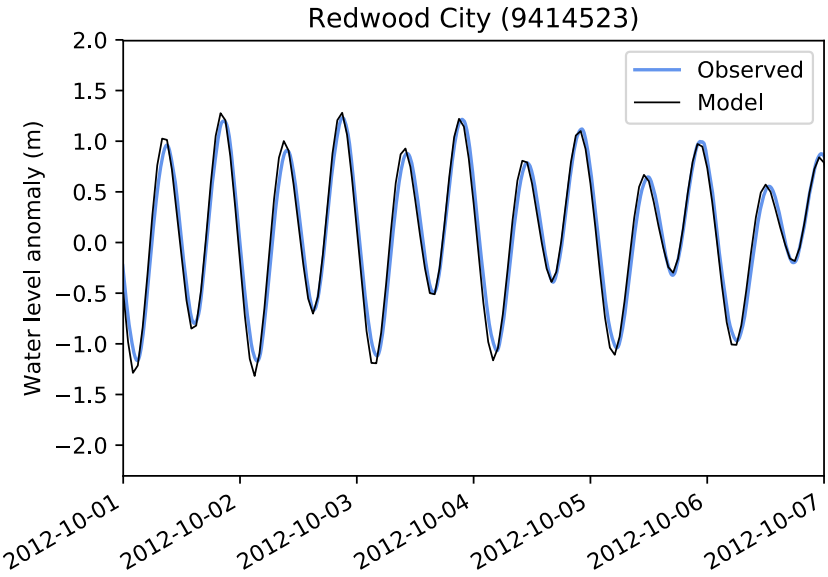

Figure 7: Water level comparison at Redwood City

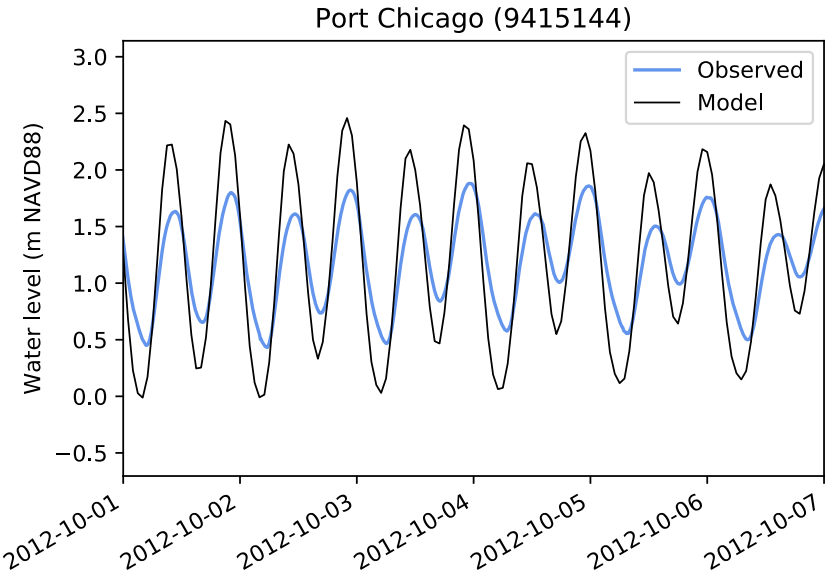

Figure 8: Water level comparison at Port Chicago

5.3 Velocity

Velocity data is taken from a series of NOAA ADCP deployments in 2012 and 2013, compiled from NOAA Tides and Currents[6]. Deployments were primarily in the summers of 2012 and 2013, with each station occupied for 1–3 months. Locations of the ADCP moorings are shown in figure 9. The unofficial compilation of the observational data used in these comparisons is also available for download[7].

Comparisons of observed and modeled velocities are presented below for the subset of the deployments that overlapped with the time period simulated. All comparisons are based on the depth-averaged observed velocity and the depth-averaged modeled velocity. Since most areas of the Bay experience linear tidal flows along a principal direction of the flow, plots and validation metrics are presented in terms of *principal* and *secondary* velocities, as opposed to east-west velocities and north-south velocities. In this context principal velocity means the velocity along the dominant orientation of the flow at the site, with the convention that positive velocity corresponds to flood-directed flow and negative velocity is ebb-directed flow. Principal velocity directions are calculated independently for each ADCP and each matching model output by maximizing variance along the principal direction. The secondary velocity direction is 90° counter-clockwise

[6] https://tidesandcurrents.noaa.gov/cdata/StationList?type=Current+Data&filter=historic&pid=34
[7] https://drive.google.com/open?id=0B9IYEz9K_uS0MTY5TFZOWEtQSEE

to the principal direction. Plots of velocity time series for both the principal and secondary components are truncated to a period of 8 days in order to keep the tidal variation and shape discernible in the plots. In addition to time series plots, model-data comparisons of principal velocity are shown in scatter plots, with the respective principal directions depicted by a pair of arrows inset in the scatter plot. The alignment of the pair of vectors indicates the agreement between observed and modeled current direction. In these scatter plots, a distribution more horizontal than the black 1:1 line indicates over-prediction of velocity, and a more vertical distribution indicates under-prediction. Time lag or lead is indicated by the point distribution tracing out an oval.

In general, we expect an estuarine hydrodynamic model to capture the timing and direction of currents very well, and generally resolve current speeds. Current speed can vary greatly over small distances, and interpreting errors in current speed requires more critical consideration of the specific deployment location as compared to water level comparisons. The emphasis of the validation is on the principal velocity. Secondary velocities are typically very small within the Bay, such that noise and errors which are small relative to the overall current speeds appear as large errors in the secondary velocity. While secondary velocity metrics are still presented, they are generally noisy and of much less concern than the principal velocities.

Timing is largely dictated by the tidal water levels, with bed friction and depth playing secondary roles. Assuming that bathymetry and tidal water levels are accurately modeled, the remaining errors in timing are largely related to friction and tidal prism. Directions of the tidal currents with the Bay are strongly forced by bathymetry, and we expect the model to capture current directions very well as long as the observations are not tucked away in an unresolved portion of the Bay. Currents outside the Bay are subject to a wider range of processes including variable winds and large scale coastal currents. We include comparisons for some of these locations, but with the simplicity of the present model's ocean boundary these comparisons are not expected to be favorable.

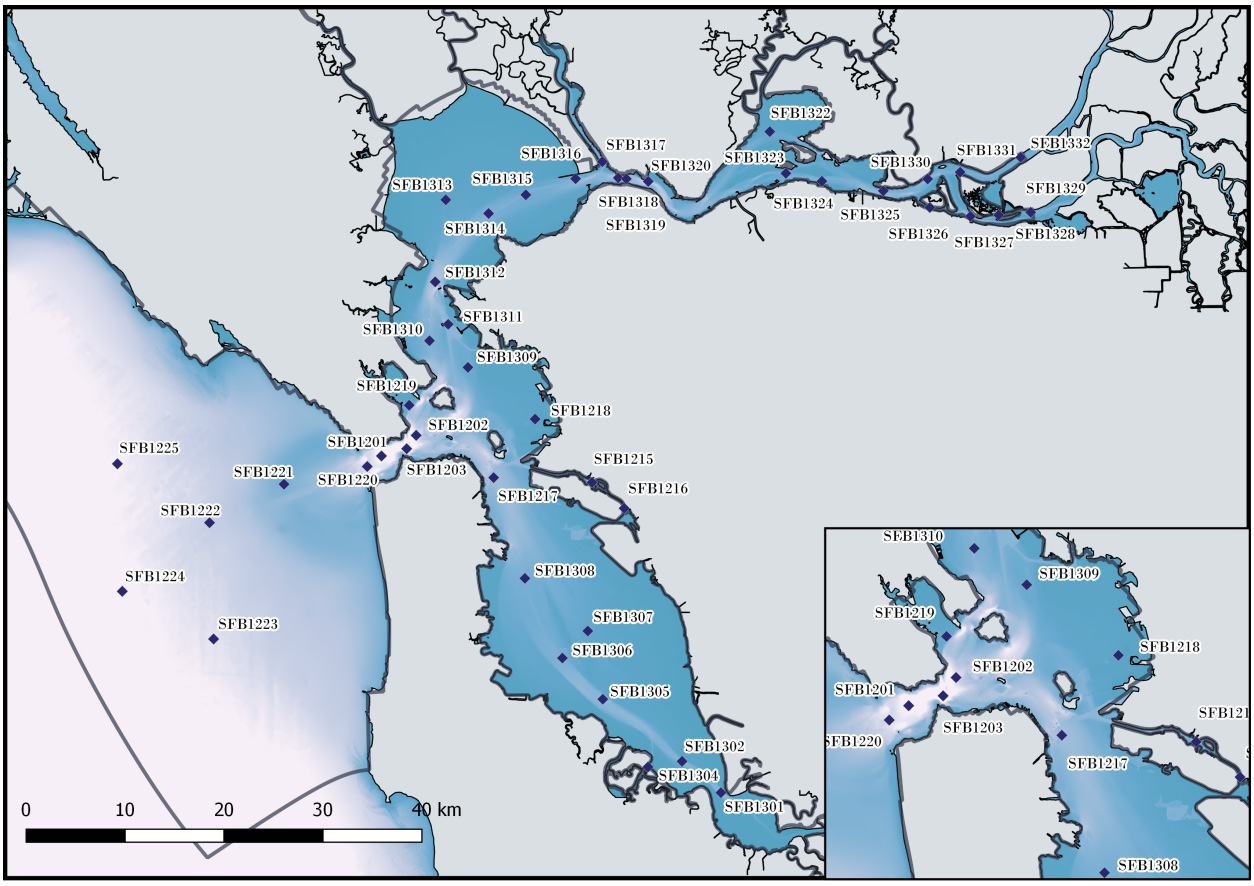

Figure 9: NOAA ADCP locations deployed during WY2013

5.3.1 South Bay

Velocity comparisons in South Bay are generally very good. In margin areas such as Redwood Creek the model is underpredicting velocity, likely due to a lack of small scale tidal prism and resolution limits in margin and slough areas. While Hunters Point appears to have a larger error in the principal velocity direction, this error has appeared across multiple models and is most likely linked to compass errors on the instrument rather than model error. The greatest errors are the velocity under-predictions at SFB1302, likely due to the relatively narrow channel mixing with adjacent shoals, and SFB1304 located in an area of under-resolved margins.

	Skill		Bias ($m\ s^{-1}$)		r^2		RMSE ($m\ s^{-1}$)		Lag (min)		Amp. factor	
Name	Pri.	Sec.	Pri.	Sec.	Pri.	Sec.	Pri.	Sec.	Pri.	Sec.	Pri.	Sec.
SFB1301	0.985	0.707	-0.013	-0.005	0.968	0.278	0.118	0.016	-15.60	8.4	0.85	0.99
SFB1302	0.973	0.562	0.050	-0.007	0.967	0.172	0.169	0.019	-14.70	8.5	0.77	0.49
SFB1304	0.920	0.520	-0.008	0.006	0.942	0.201	0.138	0.012	-20.85	9.0	0.59	0.34
SFB1305	0.984	0.447	0.055	0.065	0.959	0.085	0.126	0.077	-16.27	8.8	0.90	0.22
SFB1306	0.982	0.381	0.089	0.005	0.967	0.026	0.123	0.019	-16.50	8.1	0.95	0.32
SFB1307	0.984	0.488	-0.017	-0.021	0.942	0.066	0.083	0.037	-25.72	7.7	0.95	0.62
SFB1308	0.994	0.625	0.017	-0.005	0.989	0.226	0.075	0.022	1.27	8.7	1.11	0.56

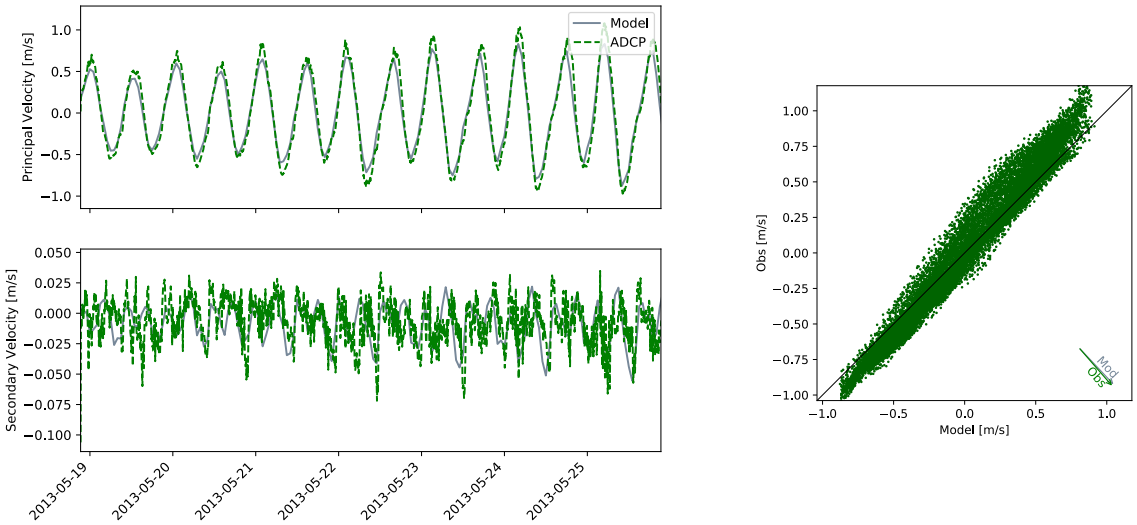

Figure 10: SFB1301 Dumbarton Bridge

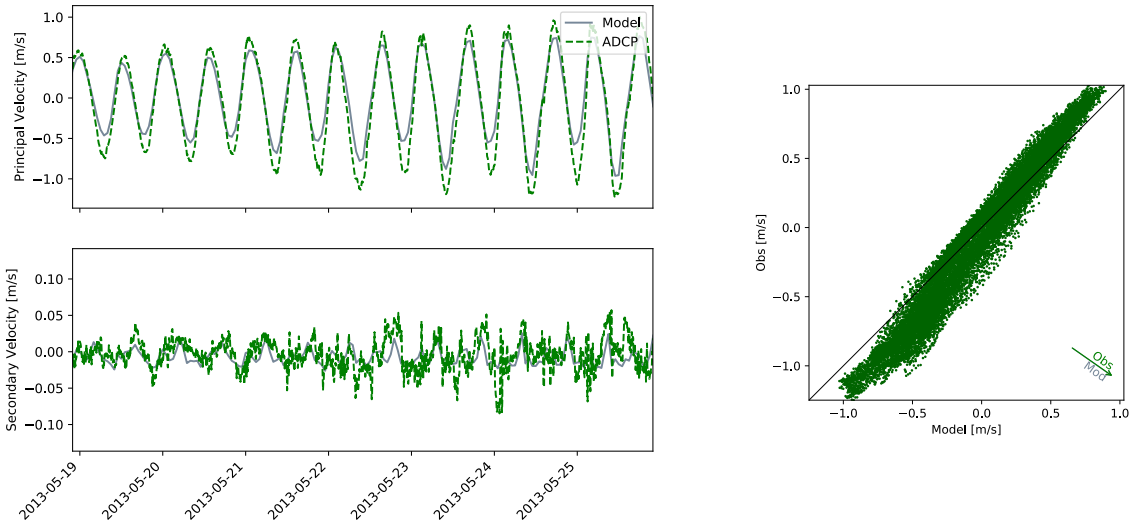

Figure 11: SFB1302 Redwood Point, 1.7 nm E of

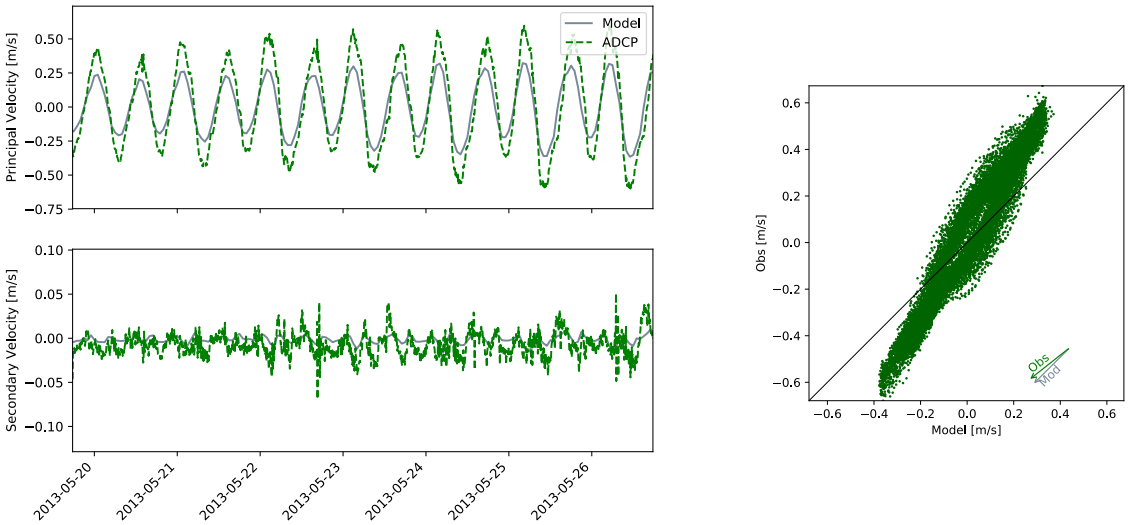

Figure 12: SFB1304 Redwood Creek

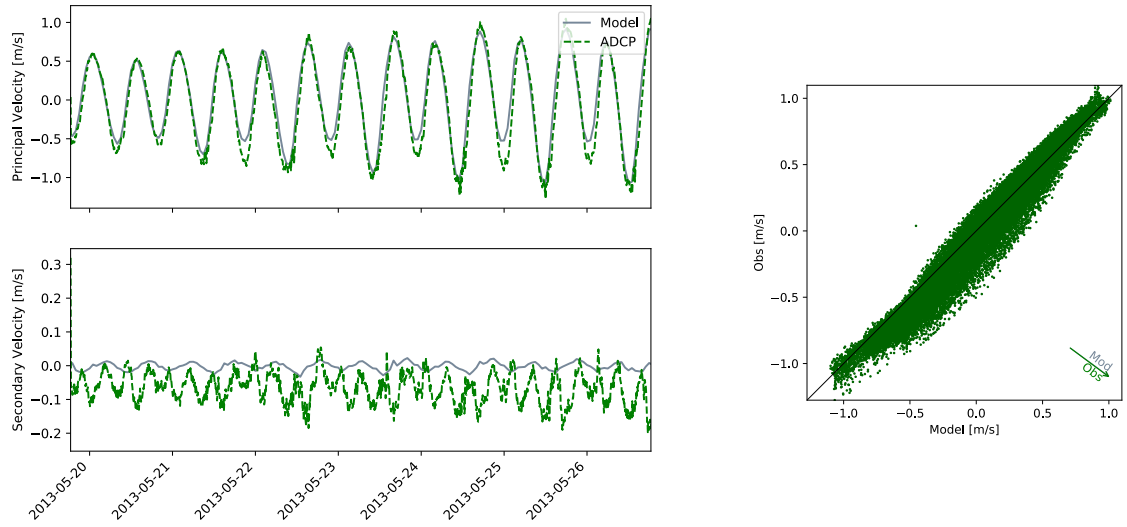

Figure 13: SFB1305 San Mateo Bridge

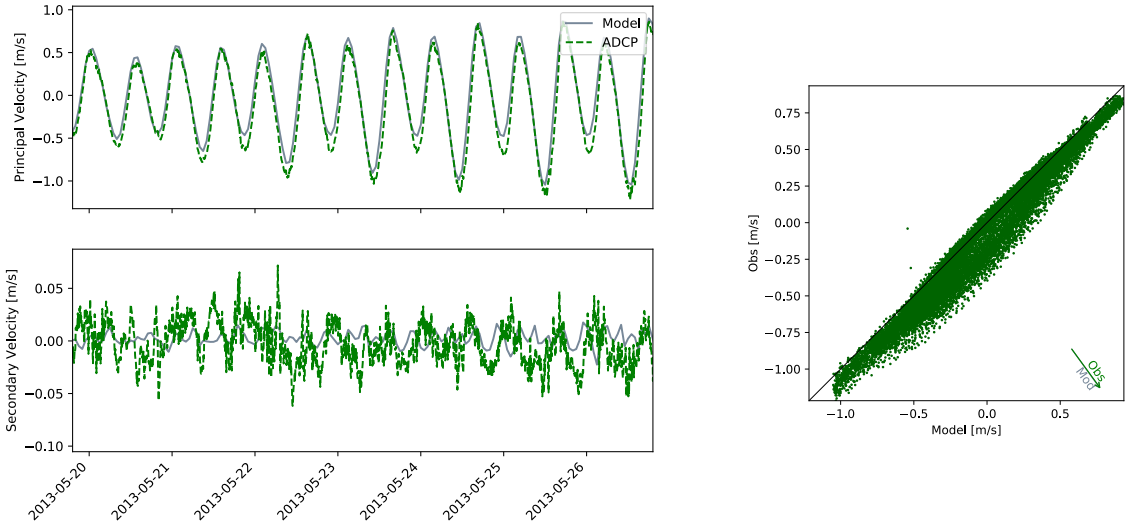

Figure 14: SFB1306 Anchorage 138

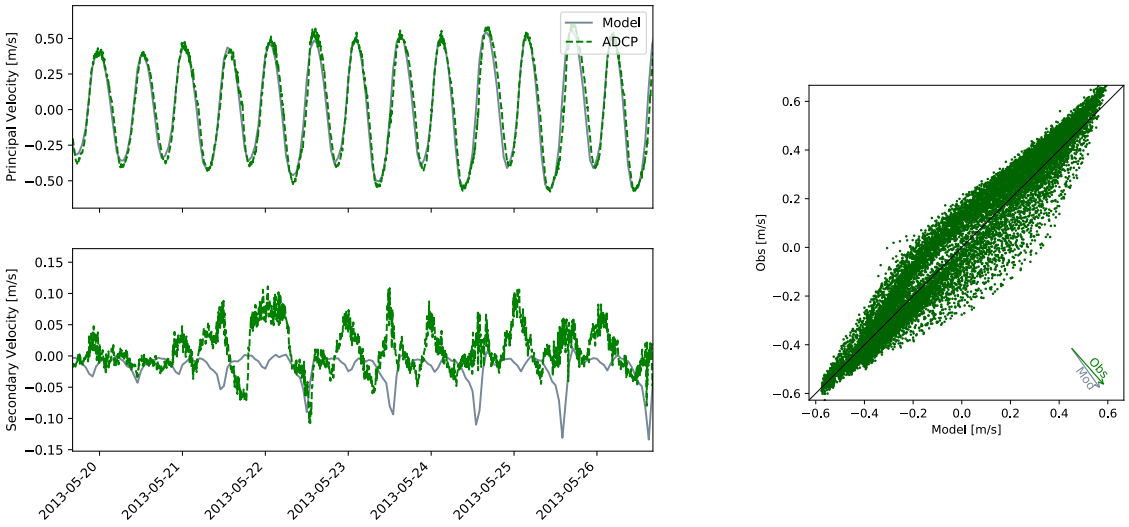

Figure 15: SFB1307 Mulford Gardens Channel Approach

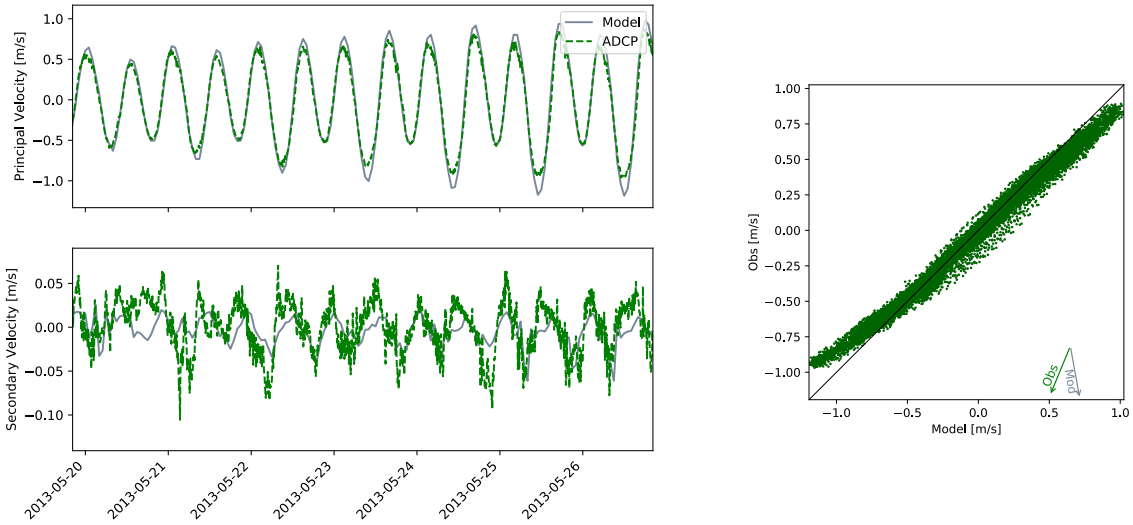

Figure 16: SFB1308 Hunters Point, 1.6 nm SE of. Compass errors in the observations are likely the cause of the difference in principal direction.

5.3.2 Central Bay

Central Bay is a particularly complex region for modeling hydrodynamics due to the high velocities, complex bathymetry, and its position at the junction of the two arms of San Francisco Bay. While velocities at Golden Gate are slightly over-represented, given the complexities of Central Bay the result here and at most open-water sites in the region is reasonably good. Previous models have shown a strong bias between tidal phases in this area, with the flood-tide jet under-represented due to horizontal numerical diffusion. The structured,

flow-aligned grid in this region is effective at reducing that effect. Margin areas like Brooklyn Basin, which are non-energetic and driven primarily by secondary flows, are a weak point of the validation in Central Bay. Similarly, Richardson Bay is an area of interest for future water quality modeling, but is poorly resolved in the present model. The complicated character of the observed velocities, including periods of near-constant velocity, suggests that spatially variable frictional control is important here. This terminal sub-basin may also be subject to wind-driven flows which are unlikely to be resolved by the model due to the low resolution of the atmospheric forcing.

	Skill		Bias ($m\ s^{-1}$)		r^2		RMSE ($m\ s^{-1}$)		Lag (min)		Amp. factor	
Name	Pri.	Sec.	Pri.	Sec.	Pri.	Sec.	Pri.	Sec.	Pri.	Sec.	Pri.	Sec.
SFB1202	0.989	0.408	-0.021	-0.021	0.968	0.005	0.160	0.086	-12.88	-15.5	1.12	0.84
SFB1215	0.948	0.226	0.003	0.005	0.881	0.001	0.041	0.018	-33.00	6.0	0.75	0.10
SFB1216	0.951	0.252	-0.028	0.001	0.933	0.005	0.144	0.009	-22.27	9.6	0.70	0.22
SFB1217	0.992	0.337	-0.020	0.002	0.968	0.002	0.121	0.037	-14.47	6.0	1.00	0.58
SFB1218	0.875	0.576	-0.022	0.015	0.902	0.175	0.050	0.032	-15.07	7.6	0.56	0.55
SFB1219	0.884	0.808	-0.009	0.004	0.679	0.532	0.135	0.062	7.27	8.4	1.36	0.65
SFB1309	0.980	0.873	0.013	-0.033	0.936	0.682	0.150	0.084	-20.40	-20.7	1.12	1.31
SFB1310	0.959	0.689	0.039	0.006	0.904	0.250	0.260	0.039	-31.42	7.6	1.29	0.83
SFB1311	0.982	0.412	-0.007	0.044	0.930	0.004	0.169	0.070	-22.20	6.1	1.03	0.48
SFB1312	0.963	0.388	-0.077	-0.014	0.911	0.007	0.343	0.041	-28.57	7.0	1.24	0.41

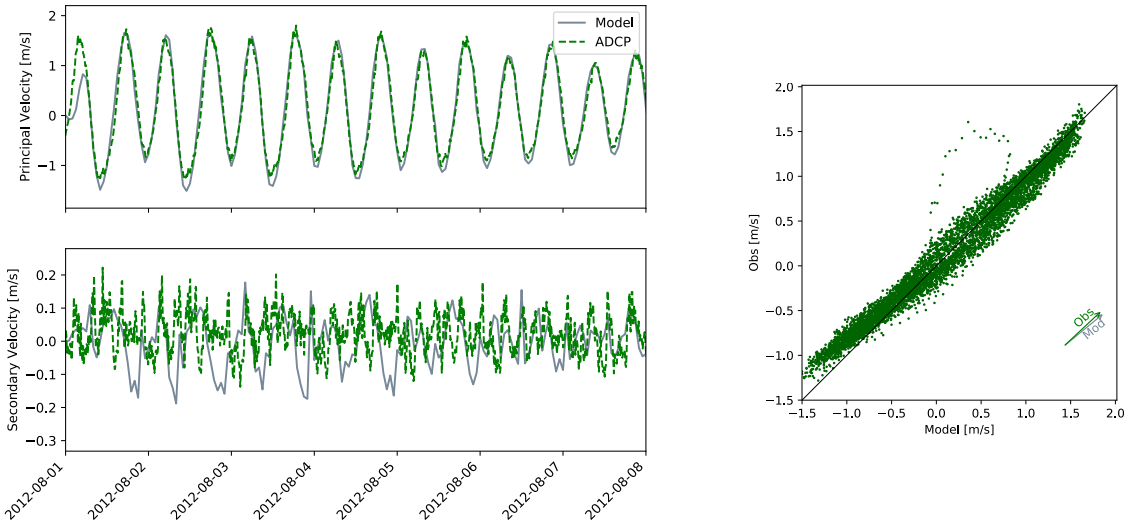

Figure 17: SFB1202 Golden Gate Bridge

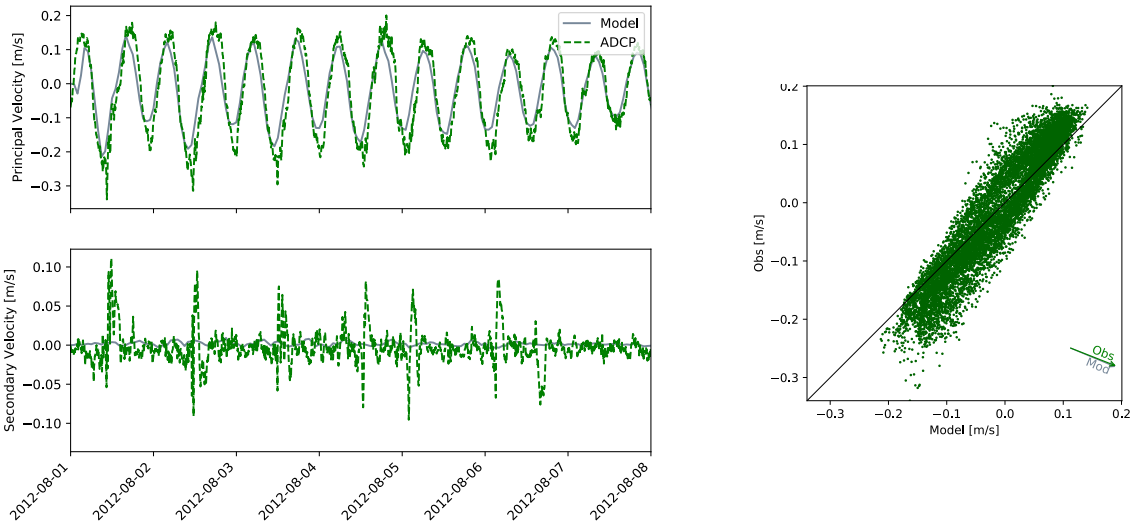

Figure 18: SFB1215 Brooklyn Basin

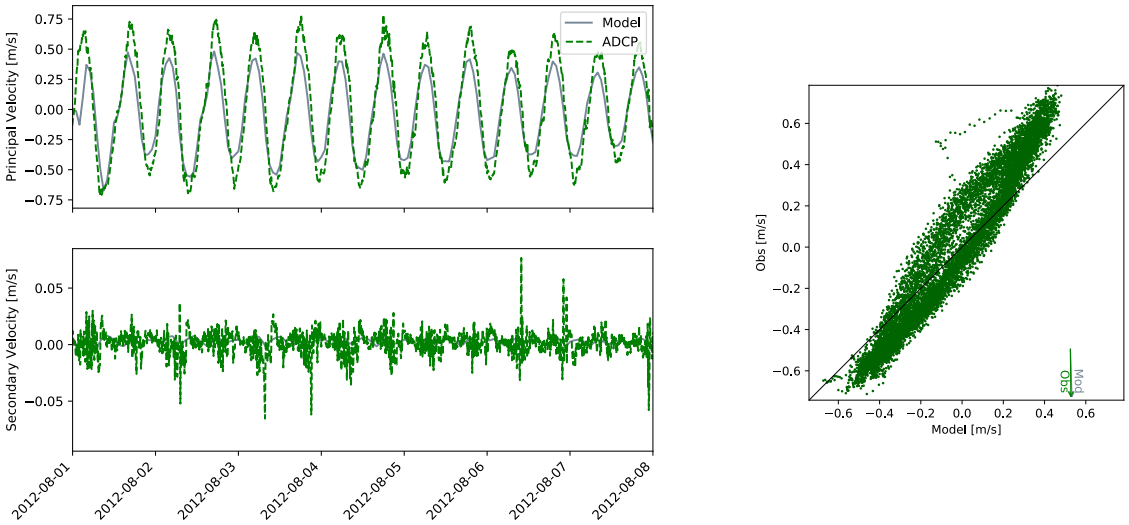

Figure 19: SFB1216 Alameda Estuary, SE End

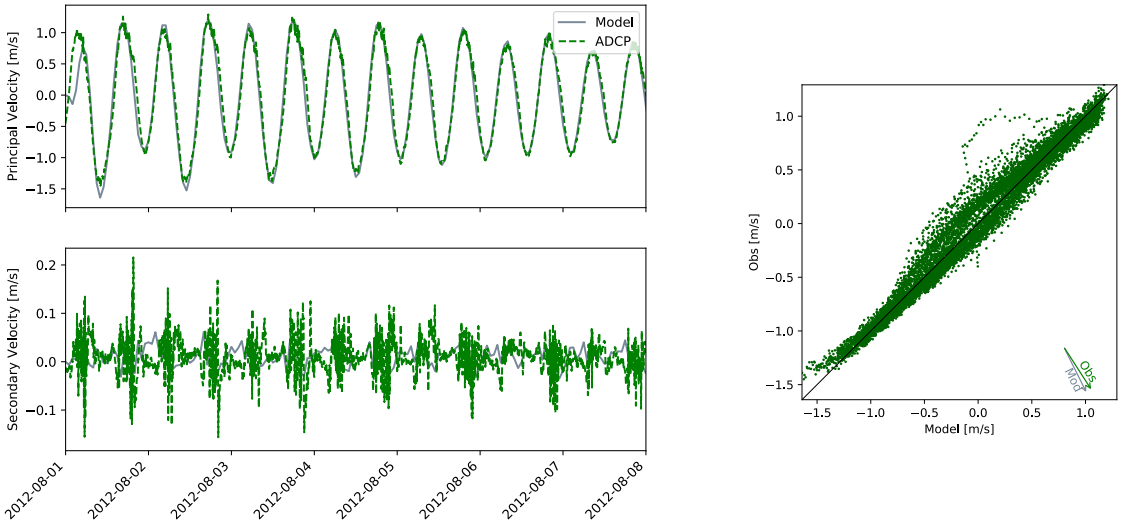

Figure 20: SFB1217 Rincon Point

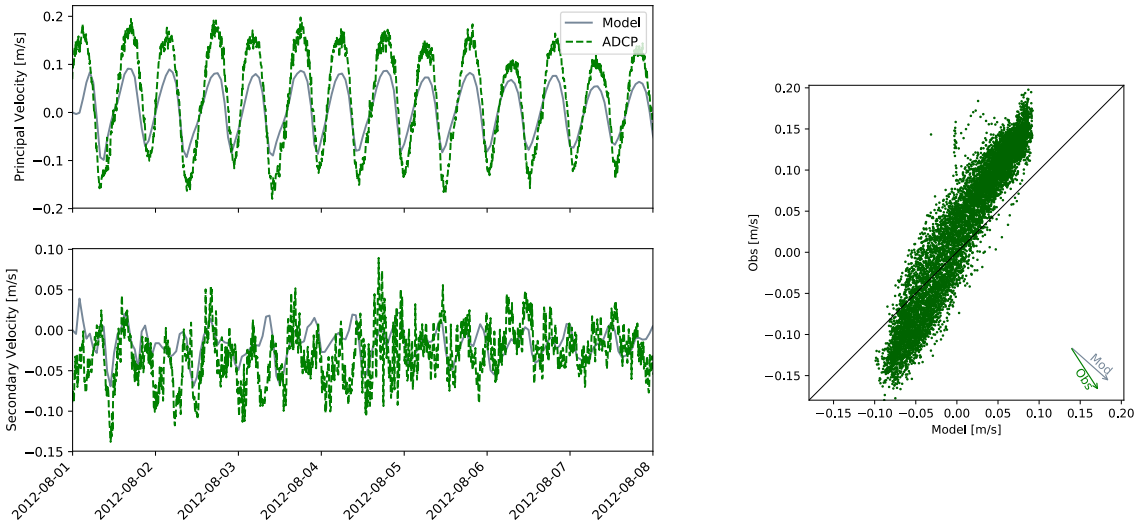

Figure 21: SFB1218 Emmeryville Marina

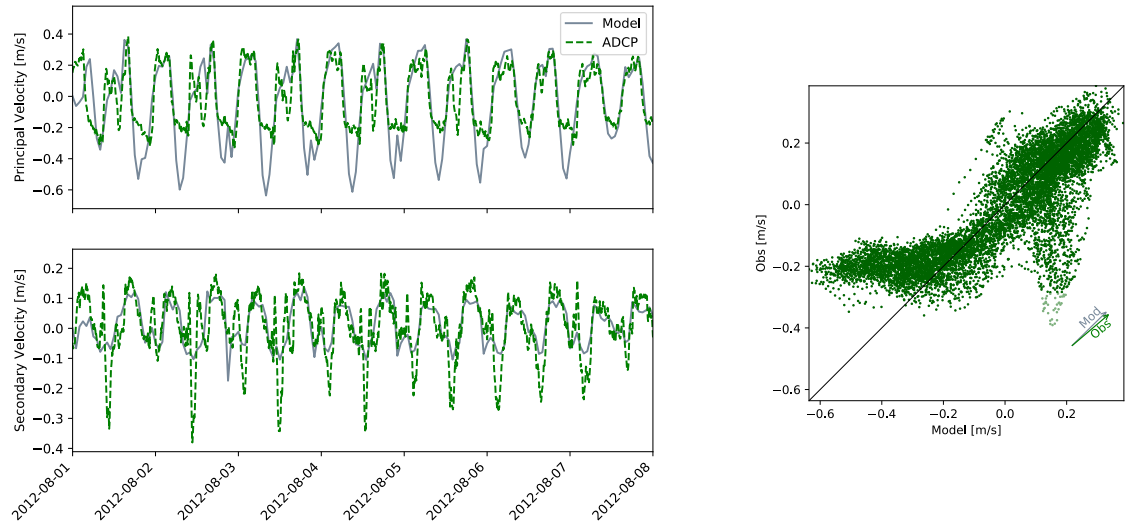

Figure 22: SFB1219 Richardson Bay

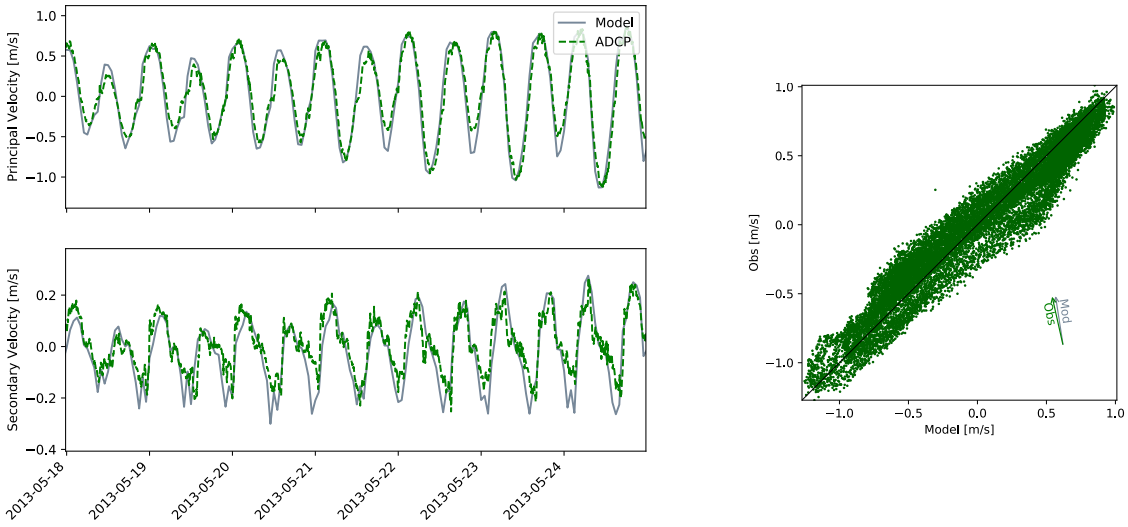

Figure 23: SFB1309 Point Chauncey, 1.3 nm E of.

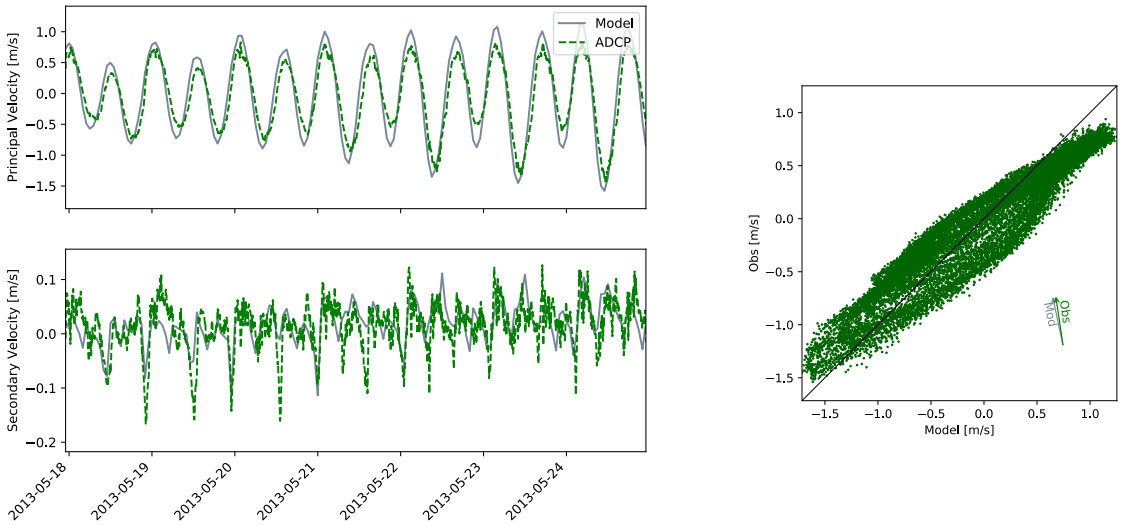

Figure 24: SFB1310 Point Chauncey, 1.25 miles N of.

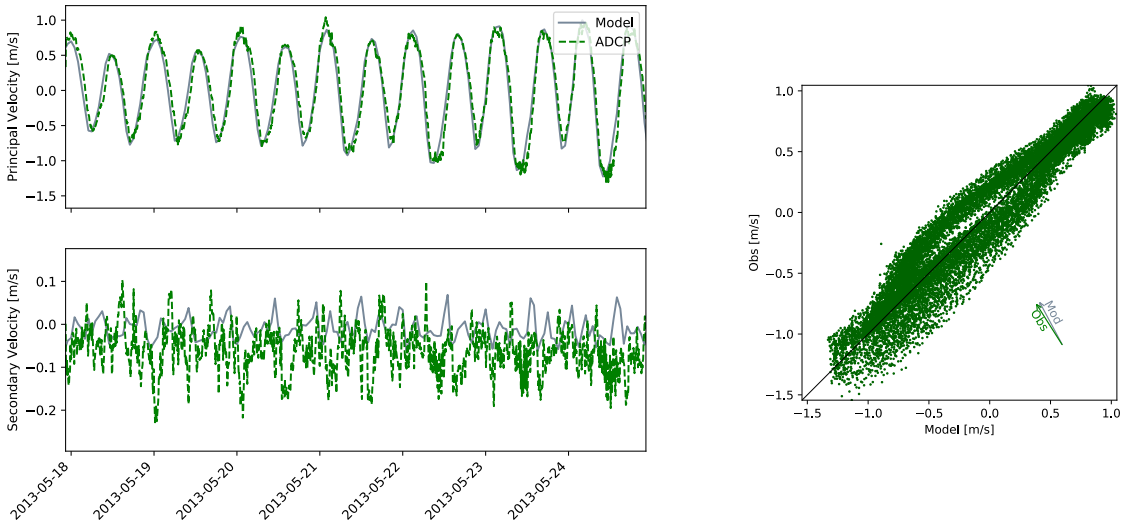

Figure 25: SFB1311 Red Rock, 0.2 nm E of.

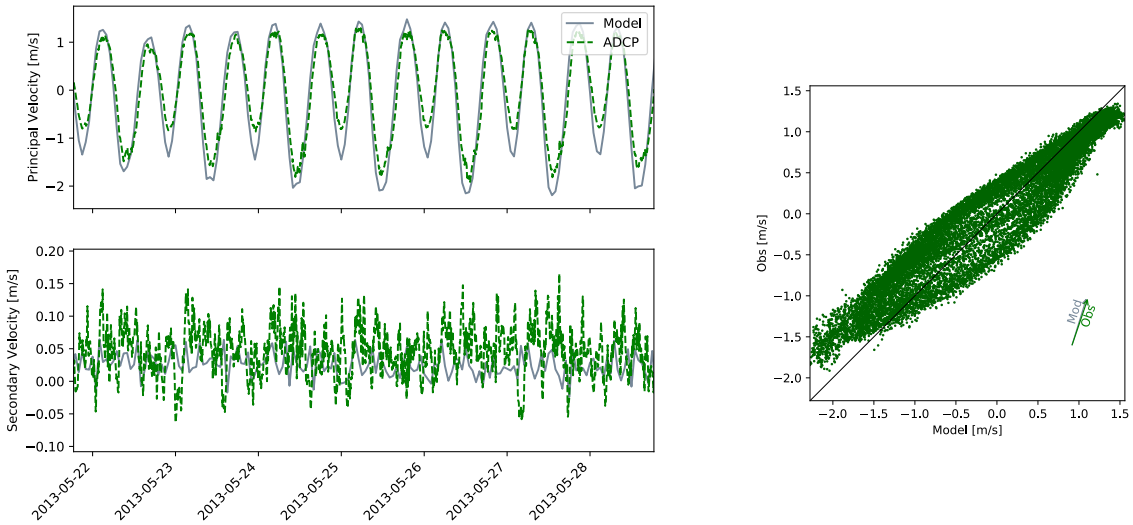

Figure 26: SFB1312 Point San Pablo, Midchannel

5.3.3 Coastal

Where station SFB1202, just inside the Golden Gate, has a small bias in overpredicting ebb, its mirror station SFB1201, just outside the Gate, has a similar bias in overpredicting floods. As opposed to the expected bias low on ebbs (i.e. an under-resolved ebb-tide jet), the error is an over-predicted flood tide. This may be related to details of the grid in this region, or may be the combined effects of an under-resolved ebb-tide jet and an overall bias high. The drivers of this bias are not entirely clear, as the comparison at the next station out, SFB1220, are quite good and presumably still sampling the ebb-tide jet. Points beyond the SF Bar

are included for completeness, but are not expected to validate given the simplicity of the ocean boundary condition.

	Skill		Bias ($m\ s^{-1}$)		r^2		RMSE ($m\ s^{-1}$)		Lag (min)		Amp. factor	
Name	Pri.	Sec.	Pri.	Sec.	Pri.	Sec.	Pri.	Sec.	Pri.	Sec.	Pri.	Sec.
SFB1201	0.977	0.492	0.062	-0.044	0.947	0.046	0.253	0.121	-14.63	13.1	1.19	1.37
SFB1220	0.994	0.801	-0.007	-0.024	0.977	0.461	0.118	0.076	-8.77	8.9	0.96	1.20
SFB1221	0.981	0.647	0.007	-0.038	0.963	0.179	0.104	0.109	-8.62	-20.5	1.22	1.07
SFB1222	0.845	0.398	-0.041	-0.065	0.594	0.010	0.084	0.105	-19.95	56.6	1.03	1.37
SFB1223	0.654	0.367	-0.021	0.004	0.203	0.001	0.097	0.059	-68.77	44.6	0.73	1.55

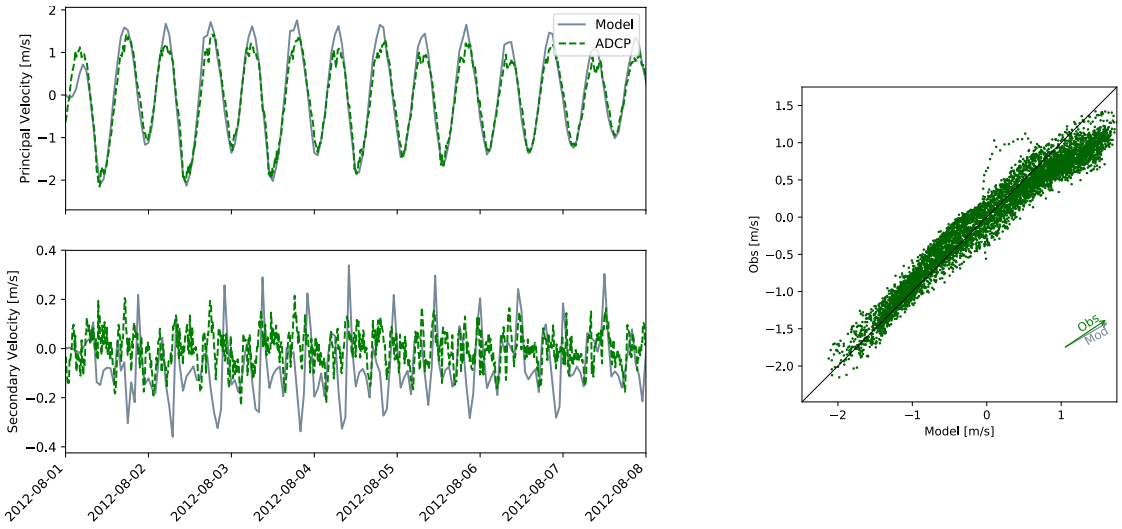

Figure 27: SFB1201 San Francisco Bay Entrance

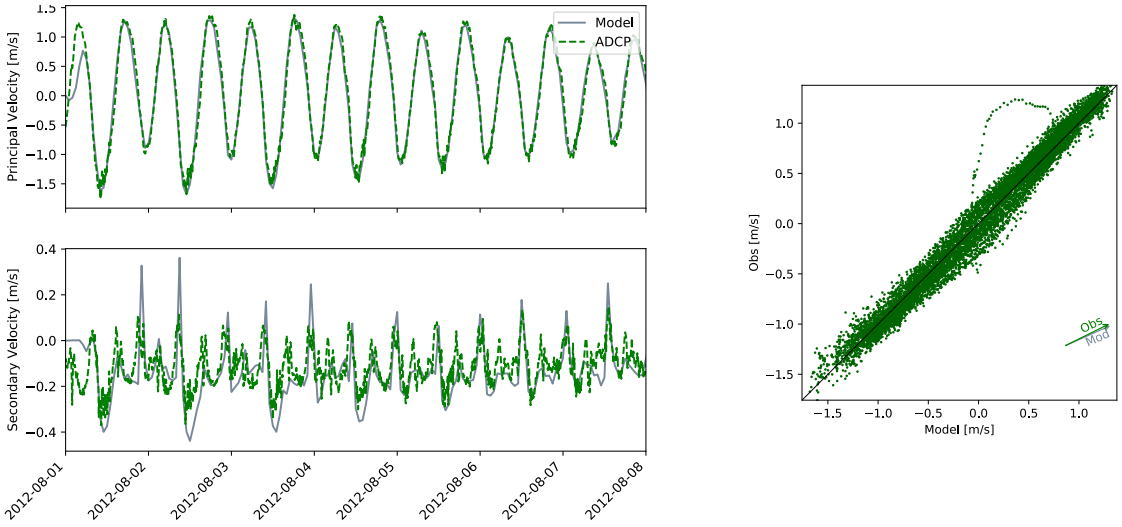

Figure 28: SFB1220 Pt Bonita, 0.95 nm SSE

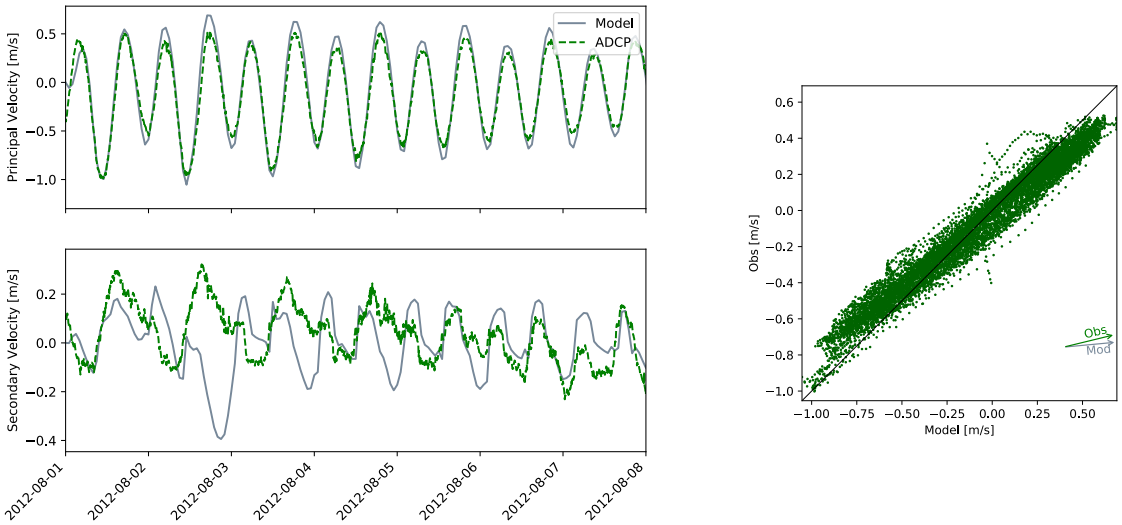

Figure 29: SFB1221 SF Bar

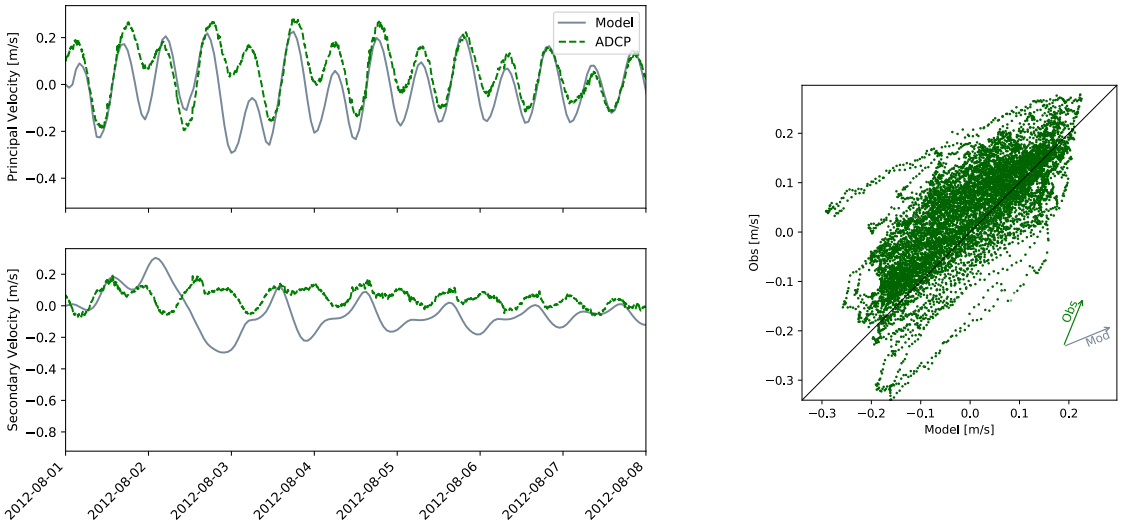

Figure 30: SFB1222 SF Buoy

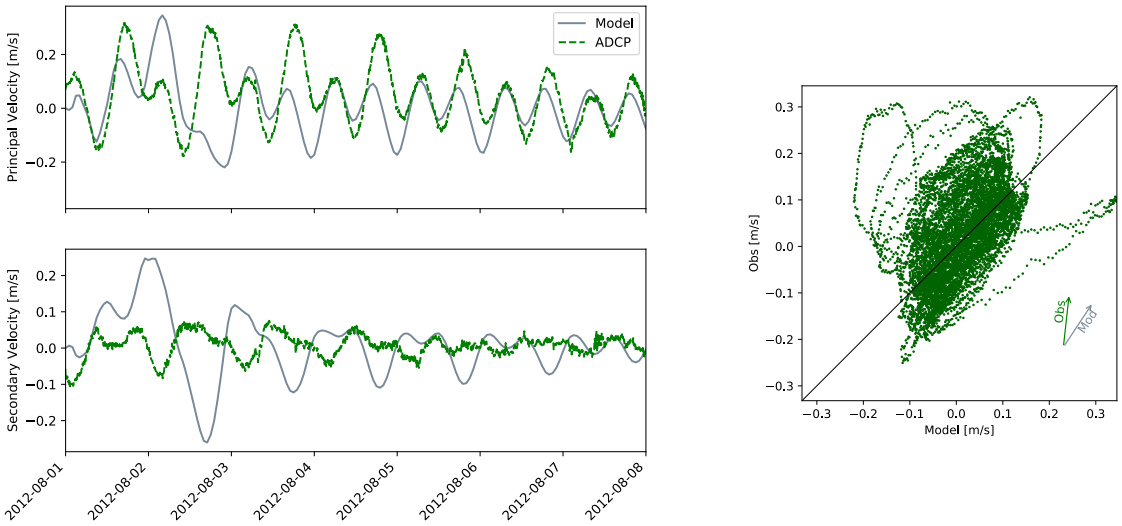

Figure 31: SFB1223 Pt. San Pedro, 8.8 SSE of

5.3.4 North Bay

The North Bay velocity comparisons are dominated by significant phase errors (the model leads the observations) and over-predicted amplitudes. The truncated Delta of this model is likely at the center of this discrepancy, as it does not adequately dampen the landward propagating tide. The tide is then free to reflect seaward, leading to overpredicted water levels near the boundary, and overpredicted velocities farther from the boundary. The phase lead of the velocity further supports this interpretation.

	Skill		Bias ($m\ s^{-1}$)		r^2		RMSE ($m\ s^{-1}$)		Lag (min)		Amp. factor	
Name	Pri.	Sec.	Pri.	Sec.	Pri.	Sec.	Pri.	Sec.	Pri.	Sec.	Pri.	Sec.
SFB1313	0.958	0.559	-0.013	-0.016	0.881	0.109	0.161	0.040	-33.97	7.2	1.23	0.76
SFB1314	0.943	0.712	0.003	-0.009	0.877	0.376	0.342	0.027	-38.25	8.0	1.37	0.61
SFB1315	0.916	0.526	0.025	0.000	0.816	0.094	0.367	0.030	6.04	8.7	1.46	0.60
SFB1316	0.905	0.376	0.024	-0.026	0.708	0.026	0.400	0.044	-67.57	6.0	1.23	0.47
SFB1317	0.244	0.407	0.023	-0.019	0.700	0.004	0.642	0.040	34.57	-98.8	0.08	0.49
SFB1318	0.871	0.371	0.048	-0.004	0.586	0.064	0.514	0.043	-81.30	9.1	1.05	0.32
SFB1319	0.849	0.428	-0.014	-0.074	0.528	0.004	0.639	0.115	-87.52	-74.5	1.05	0.30
SFB1320	0.813	0.321	0.049	-0.010	0.535	0.000	0.423	0.061	-81.45	-75.1	1.48	0.37
SFB1322	0.774	0.540	0.020	-0.035	0.361	0.199	0.291	0.106	-105.00	-116.8	1.09	0.42
SFB1323	0.883	0.335	0.008	0.006	0.616	0.004	0.330	0.027	-75.60	87.1	0.92	0.54
SFB1324	0.873	0.534	-0.024	0.003	0.633	0.206	0.323	0.034	-74.25	6.5	0.77	0.40
SFB1325	0.846	0.148	-0.005	-0.001	0.801	0.089	0.373	0.026	-46.05	6.0	0.52	0.40
SFB1326	0.872	0.255	0.051	0.001	0.901	0.014	0.294	0.016	-14.85	7.9	0.52	0.22
SFB1327	0.922	0.372	0.011	-0.008	0.947	0.000	0.243	0.019	20.10	6.0	0.59	0.57
SFB1328	0.895	0.351	0.048	-0.008	0.959	0.001	0.247	0.019	21.07	6.0	0.54	0.09
SFB1329	0.939	0.409	-0.060	-0.006	0.878	0.008	0.193	0.020	33.45	9.7	0.74	0.70
SFB1330	0.804	0.319	0.001	-0.009	0.847	0.049	0.333	0.030	-32.17	9.0	0.43	0.17
SFB1331	0.821	0.494	0.007	0.003	0.839	0.026	0.298	0.021	-33.30	9.5	0.46	1.27
SFB1332	0.943	0.296	-0.016	-0.003	0.969	0.013	0.156	0.011	16.35	8.9	0.64	0.27

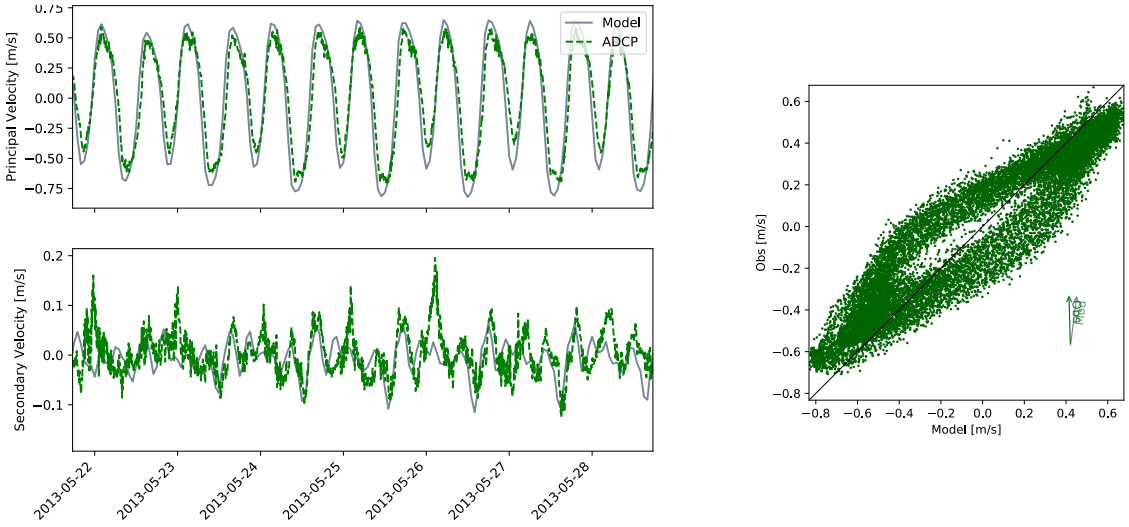

Figure 32: SFB1313 Petaluma River approach (Buoys 3 and 4)

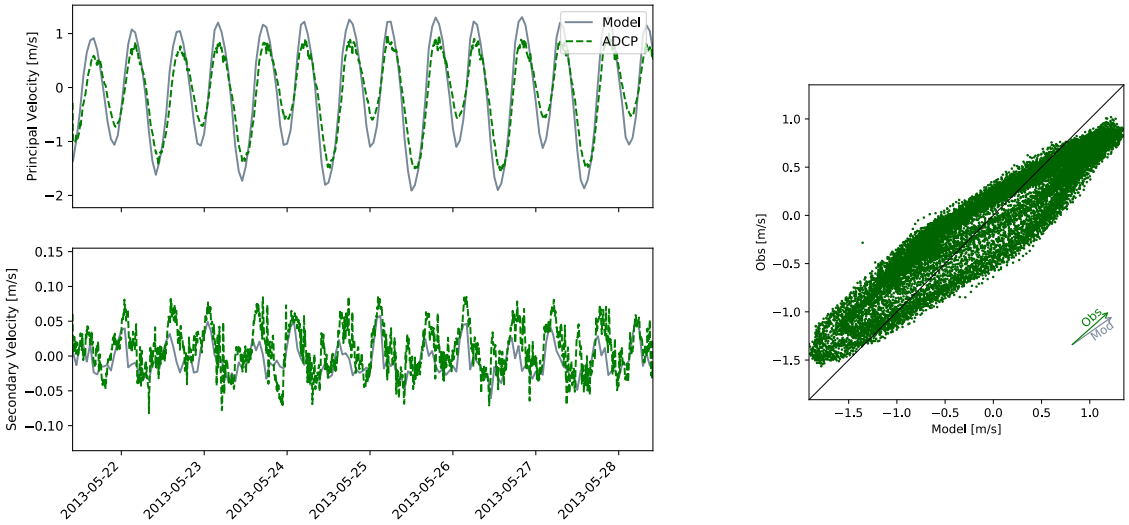

Figure 33: SFB1314 Pinole Point, 1.27 nmi. NNW of

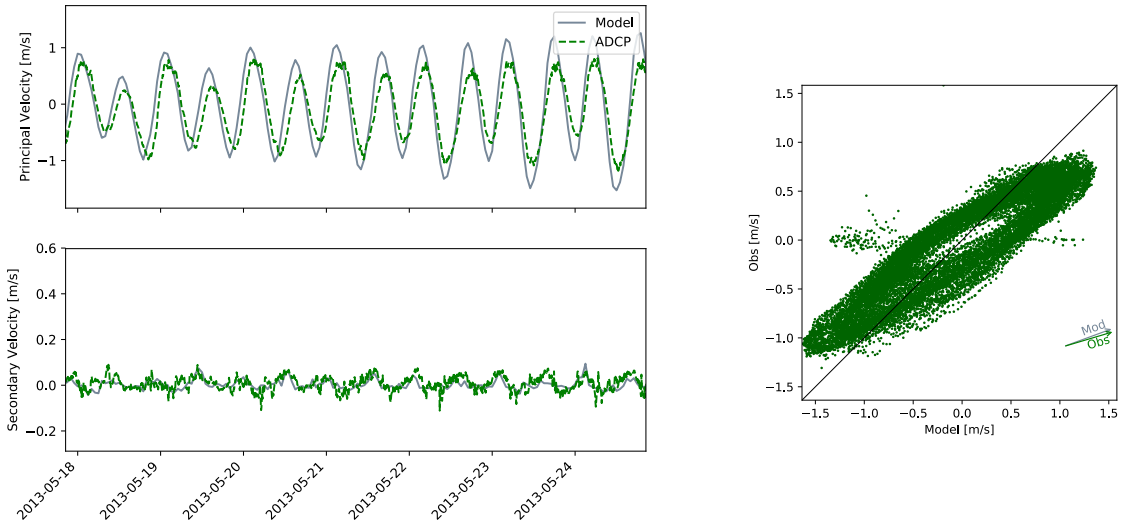

Figure 34: SFB1315 Pinole Shoal

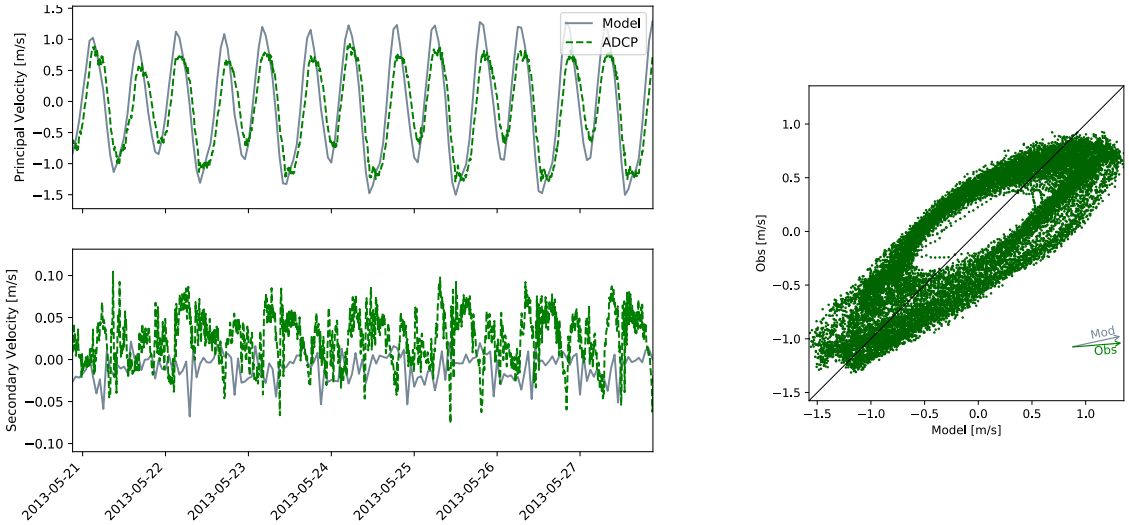

Figure 35: SFB1316 Davis Point, 1.0 nmi. NW of

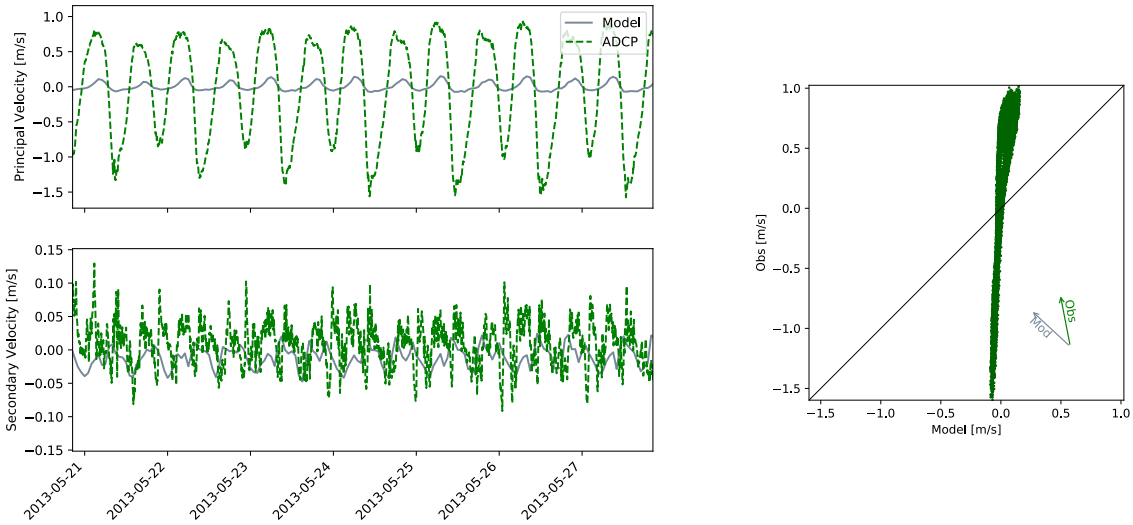

Figure 36: SFB1317 Mare Island Strait, Pier 34, NE of

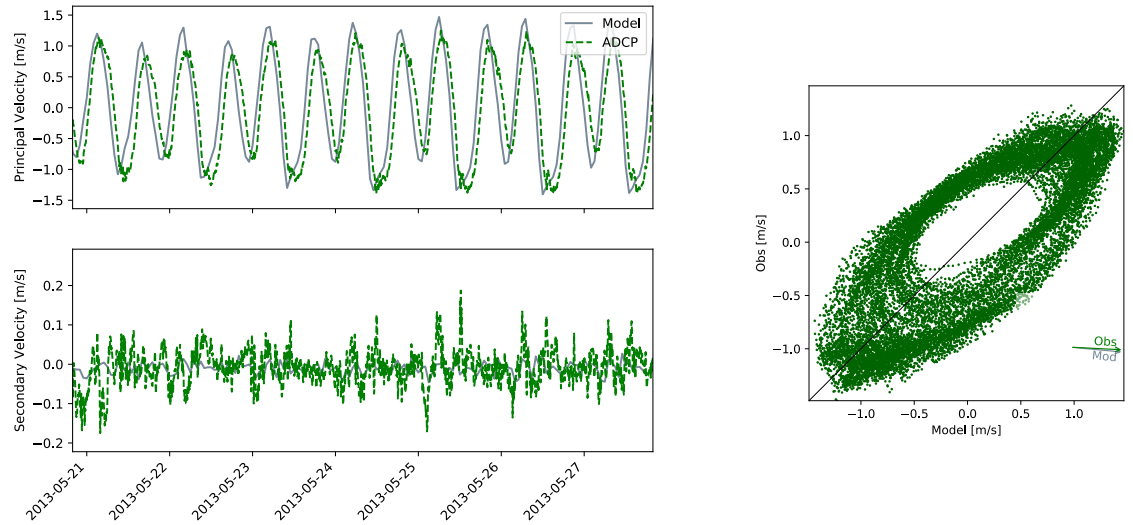

Figure 37: SFB1318 I-80 Carquinez Bridge

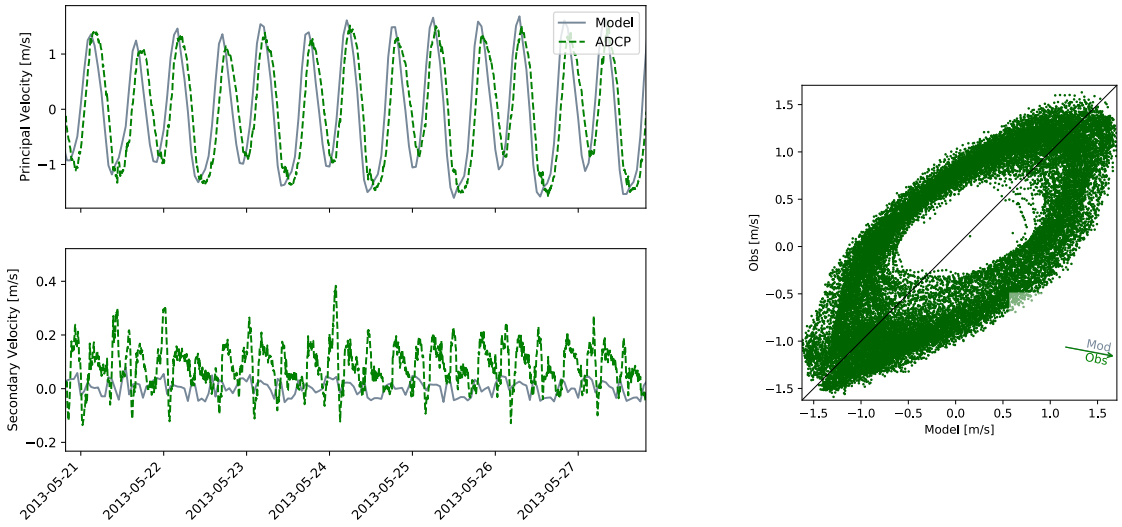

Figure 38: SFB1319 Carquinez Strait

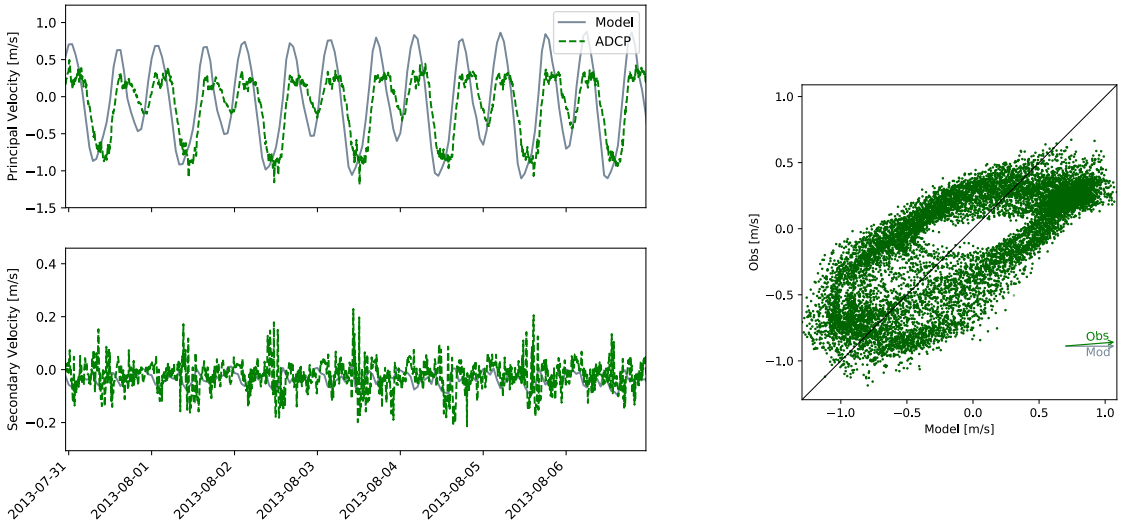

Figure 39: SFB1320 Dillon Point

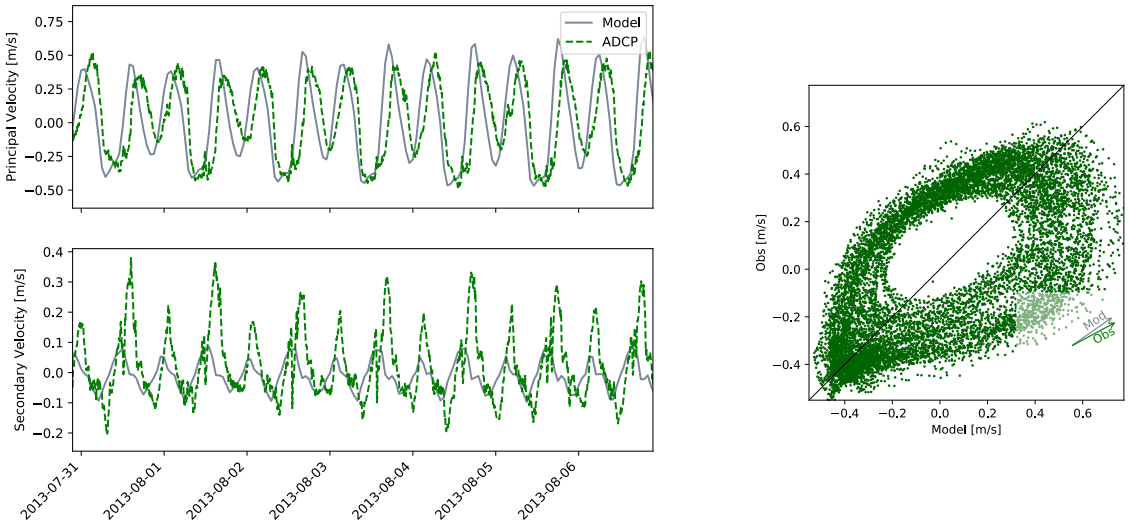

Figure 40: SFB1322 Grizzly Bay, entrance

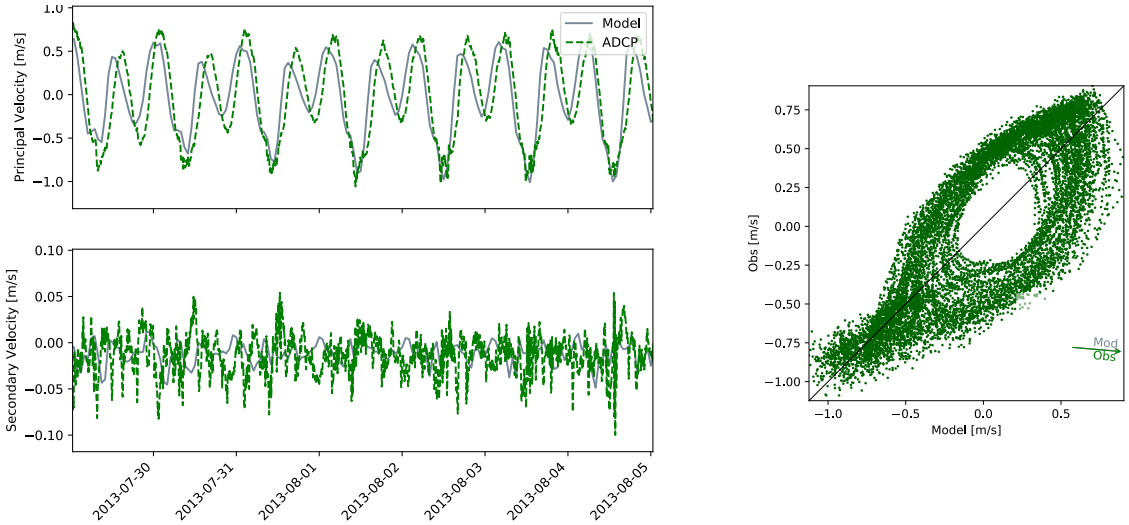

Figure 41: SFB1323 Roe Island Channel

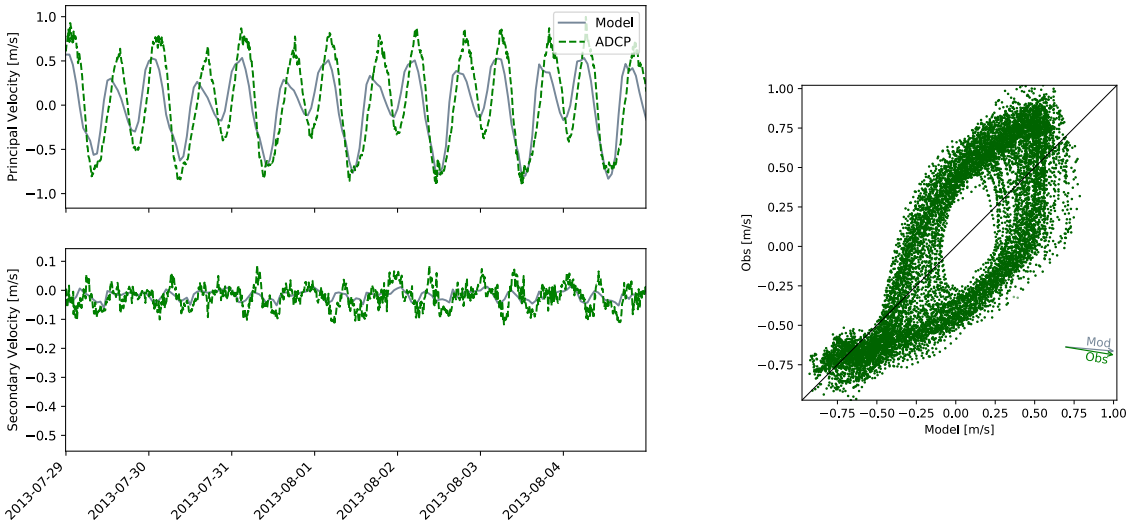

Figure 42: SFB1324 Middle Point Lt., 0.18 nmi. NNW of

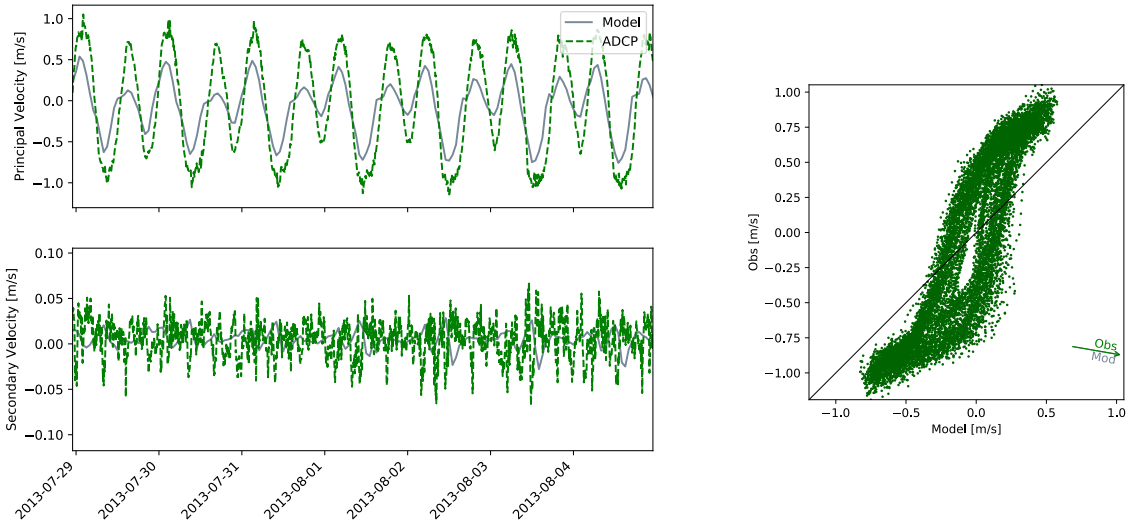

Figure 43: SFB1325 Simmons Point 0.6 nm ESE of

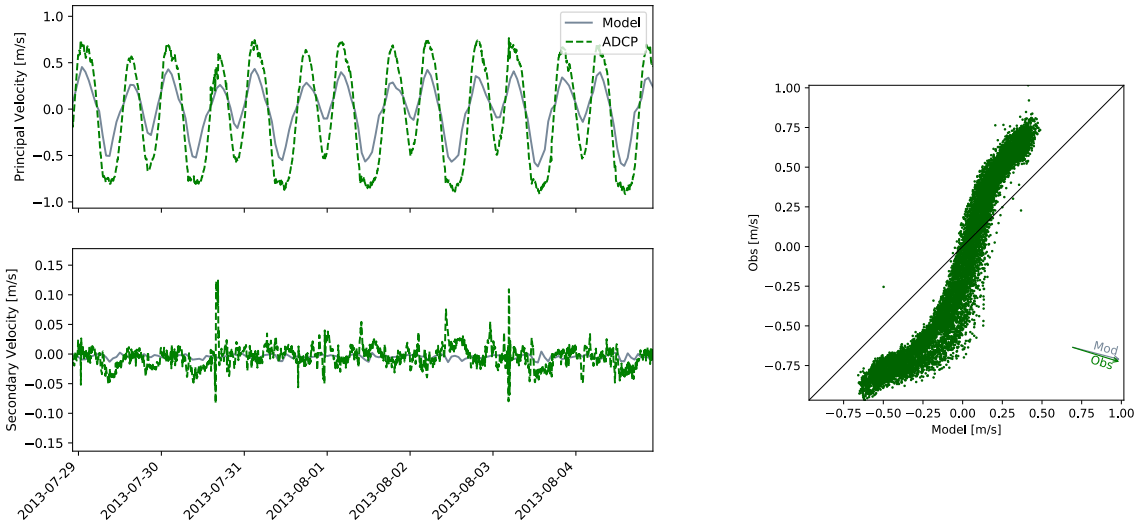

Figure 44: SFB1326 New York Slough

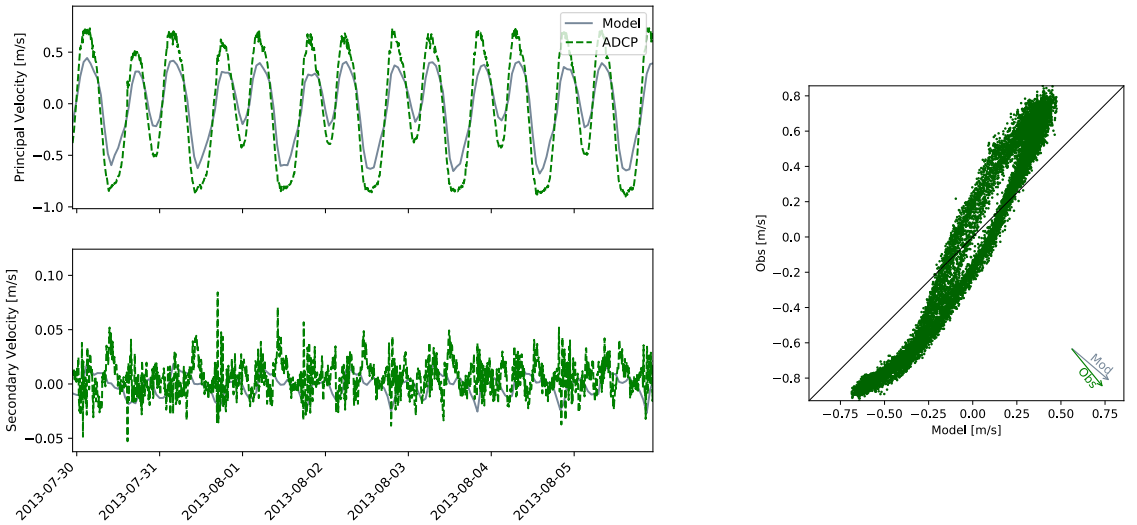

Figure 45: SFB1327 Antioch Point

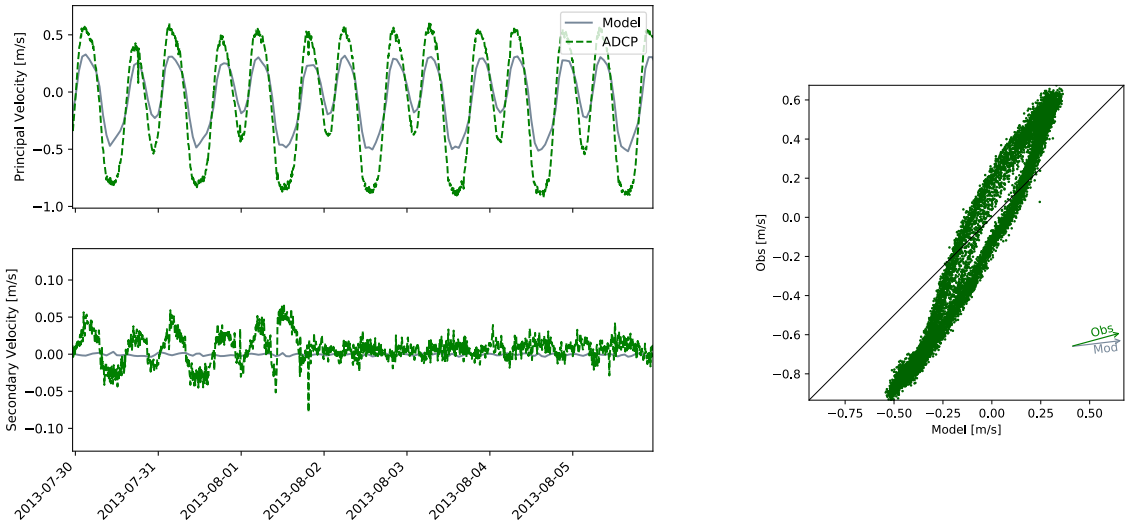

Figure 46: SFB1328 West Island, N of

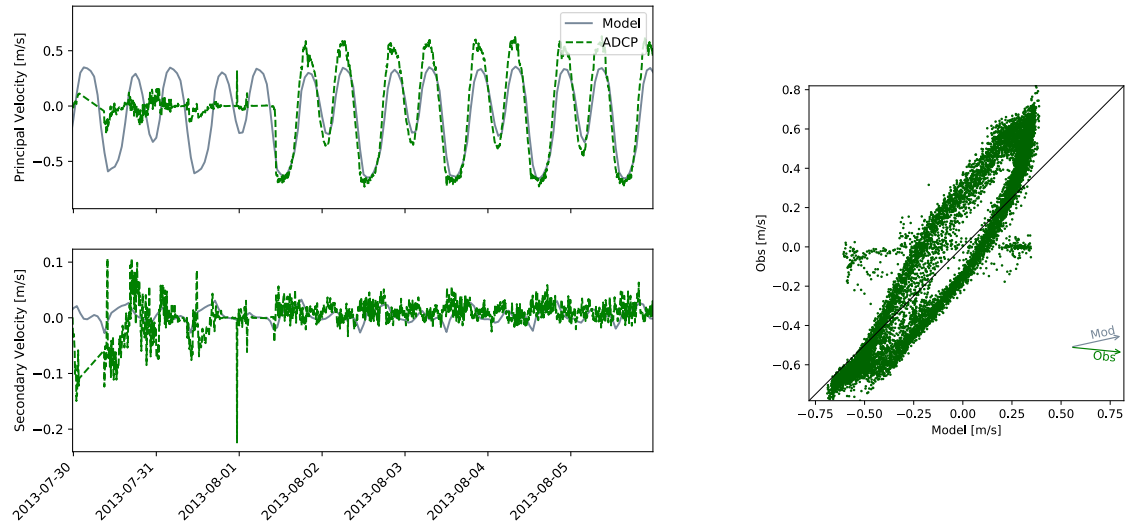

Figure 47: SFB1329 Route 160 Bridge

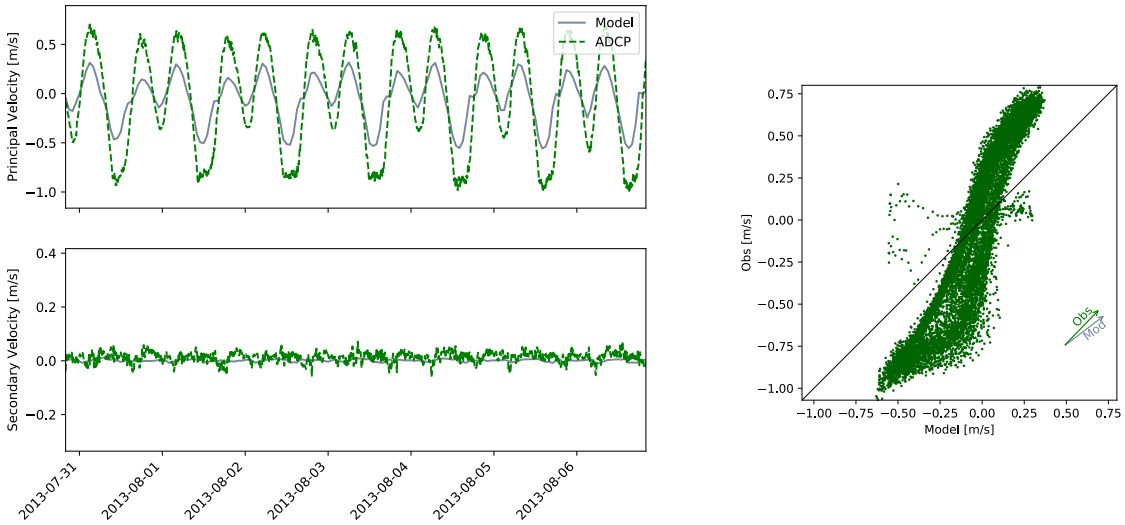

Figure 48: SFB1330 Sacramento River Entrance, 0.7nm SW of Chain Island

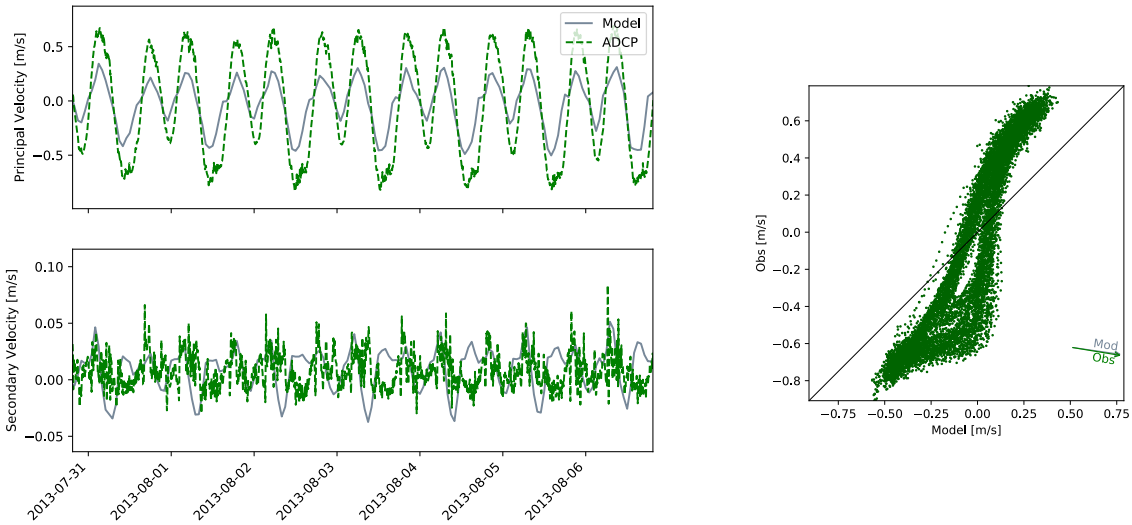

Figure 49: SFB1331 Point Sacramento, 0.2 nm NE of

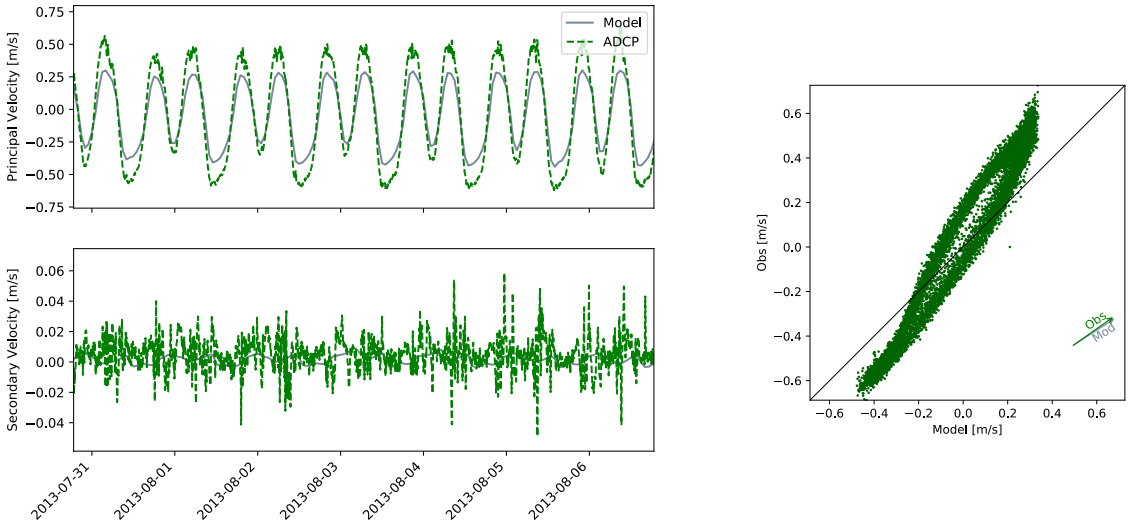

Figure 50: SFB1332 Sacramento River, Light 14

5.4 Salinity

Accurately predicting salinity is important both as a diagnostic for transport and as a driver for hydrodynamic circulation. We compare the model's output to two USGS data sources: periodic transects along the thalweg of the Bay and four moored sensors providing continuous, 15-minute data.

5.4.1 Transects

The USGS completes a cruise along the transect of the Bay on a monthly to bimonthly basis taking water property measurements at 36 stations (fig. 51). We validate our modeled salinity field against these monthly cruises, comparing both depth-averaged salinity and estimated stratification. Although some USGS cruises cover only the South Bay, we include plots of model output for the full Bay in all cases for consistency and context. Depth-averaged salinity in both the model output and observations is calculated as a simple mean of the samples within each vertical profile. Stratification is calculated within each profile as

$$\frac{\partial s}{\partial z} \approx \frac{s_{max} - s_{min}}{/} z_{max} - z_{min}$$

, essentially enforcing stable or neutral stratification. Transects are plotted south to north, with Lower South Bay on the left and the Sacramento River on the right. Thin black lines denote 5 ppt contours, with more subtle color shifts at 1 ppt intervals. The vertical dimension from the model output has been adjusted to

depth below the surface. There is some variation of the profile of the bed elevation between the observations and the model due to differences in the exact location of the observations, and bathymetric details which are not resolved in the model.

In general the model performs well, with a good representation of the stratification and shape of the longitudinal salinity profile. There is a persistent bias low during low-flow periods. The causes of this bias are being investigated, and likely related to a combination of evaporation, Delta boundary condition, and insufficient flushing in the coastal ocean.

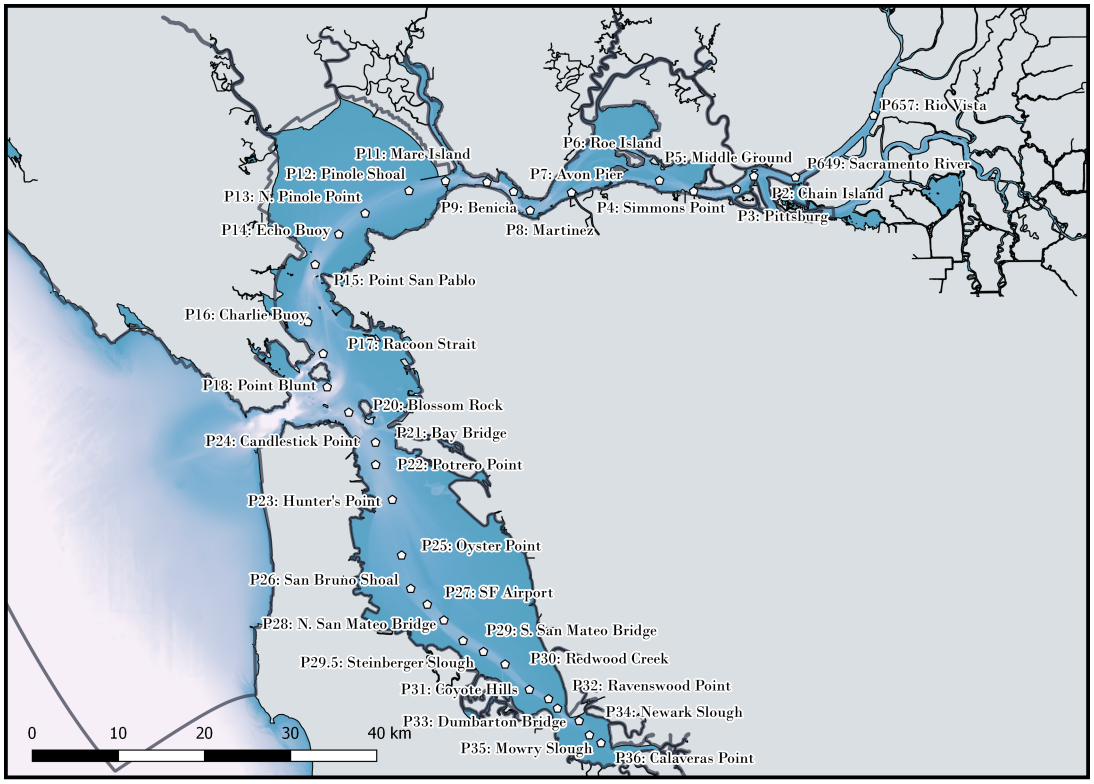

Figure 51: Locations of USGS stations during transect cruises

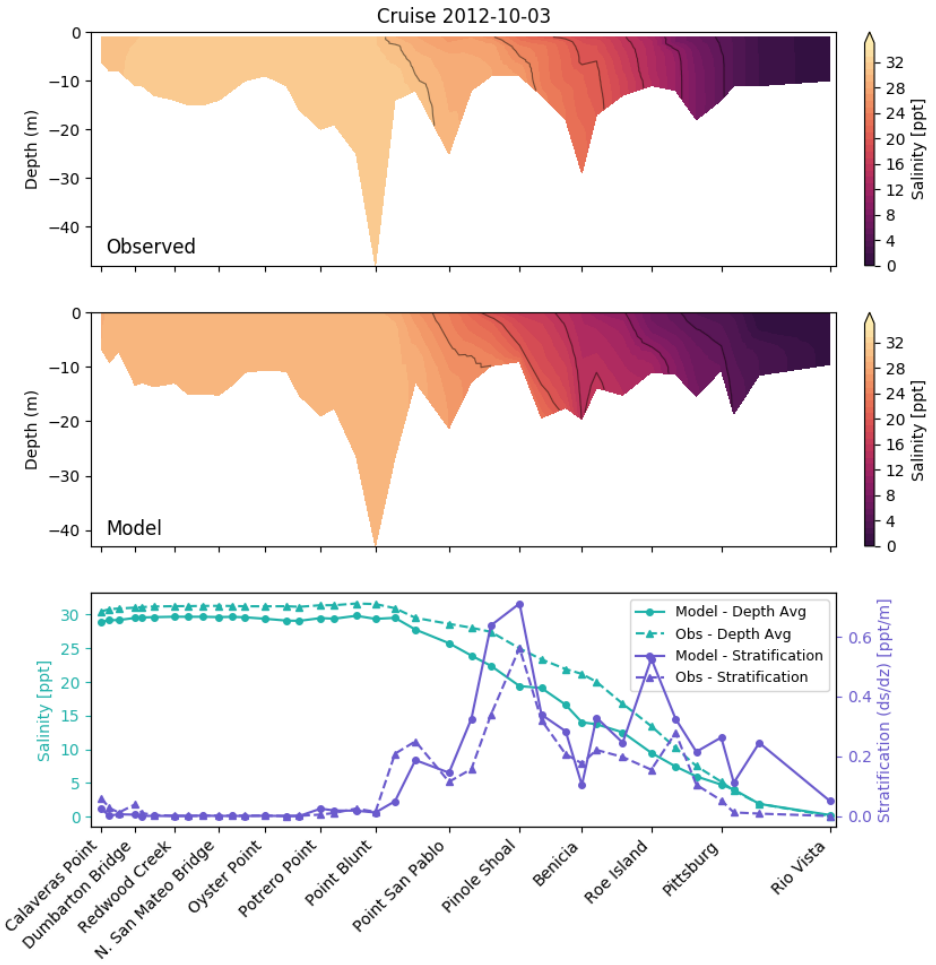

Figure 52: USGS Transect, 2012-10-03

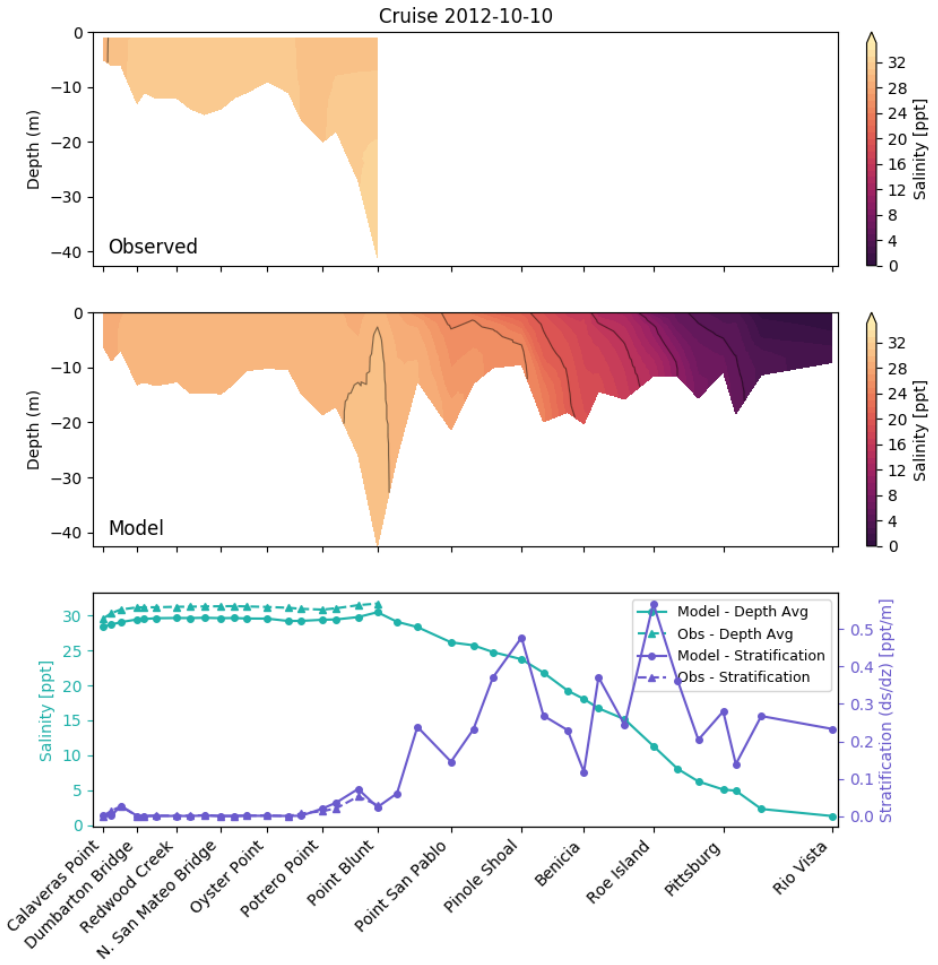

Figure 53: USGS Transect, 2012-10-10

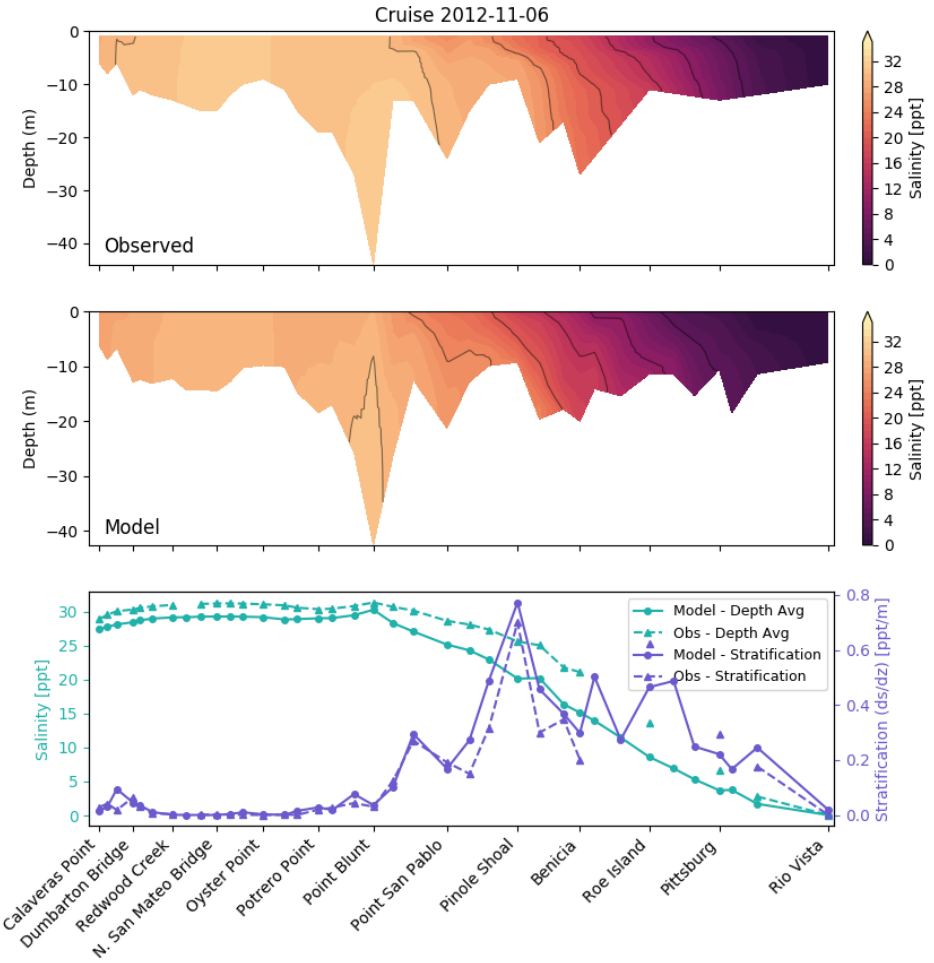

Figure 54: USGS Transect, 2012-11-06

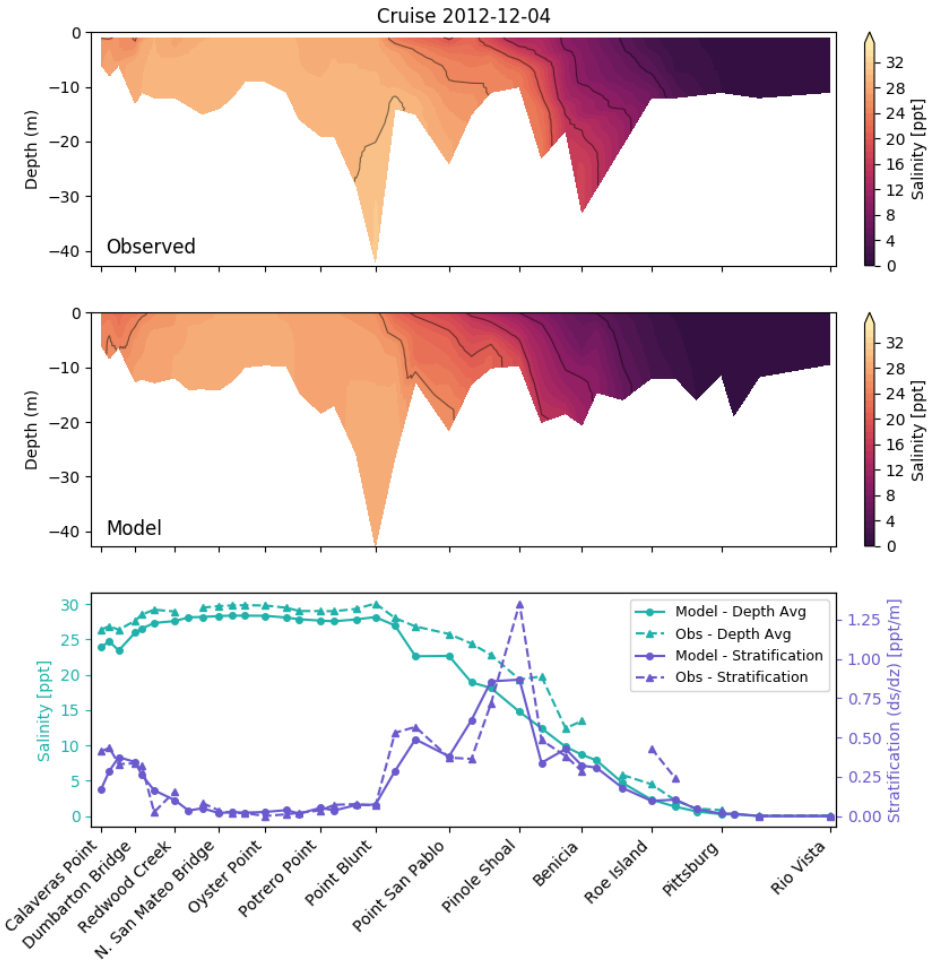

Figure 55: USGS Transect, 2012-12-04

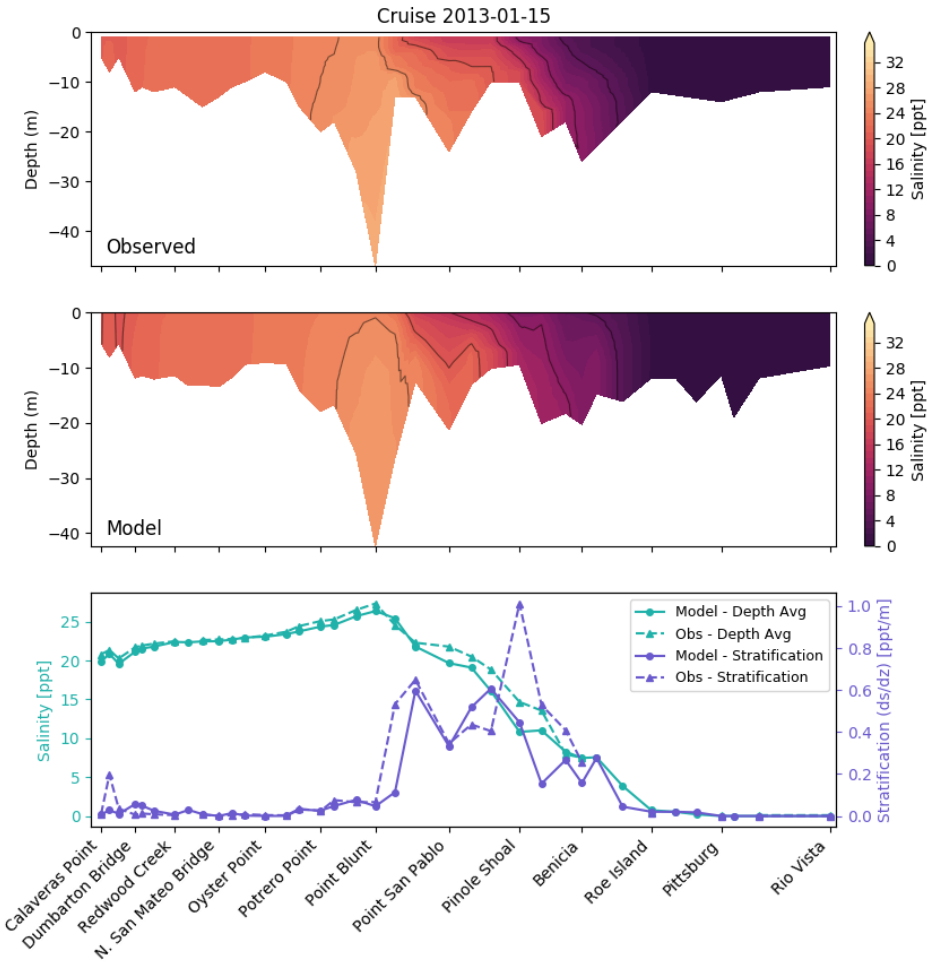

Figure 56: USGS Transect, 2013-01-15

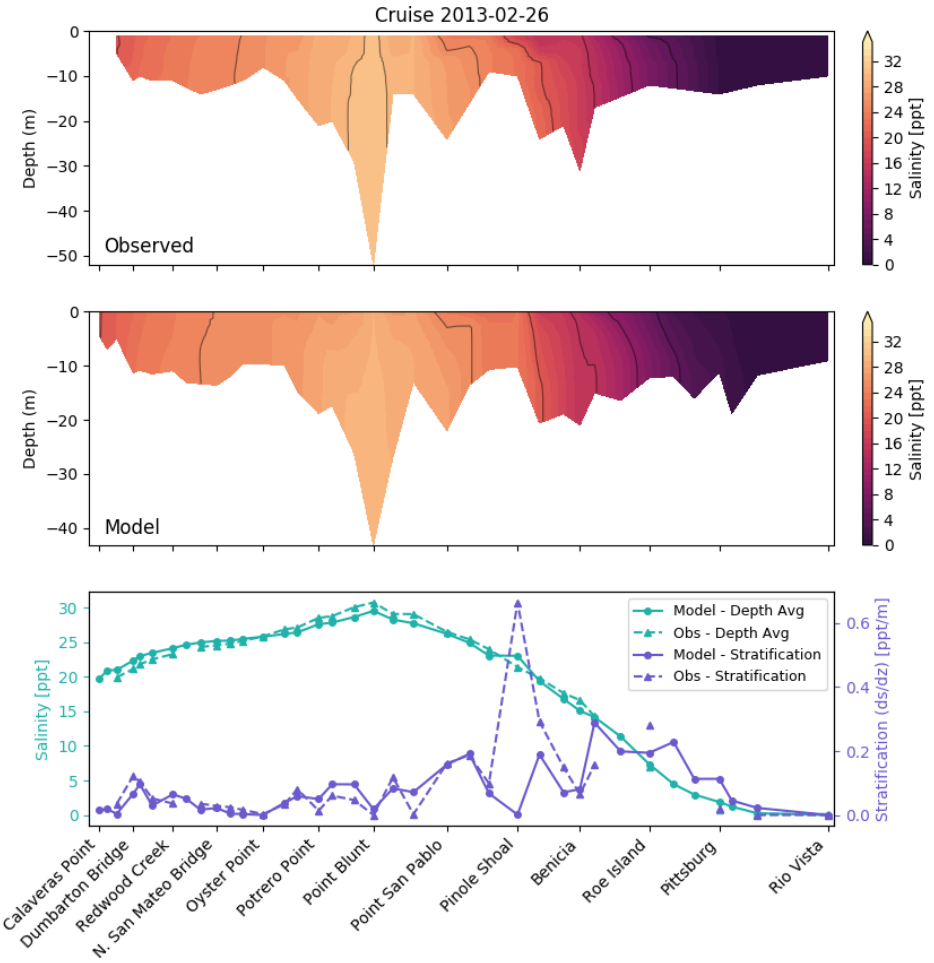

Figure 57: USGS Transect, 2013-02-26

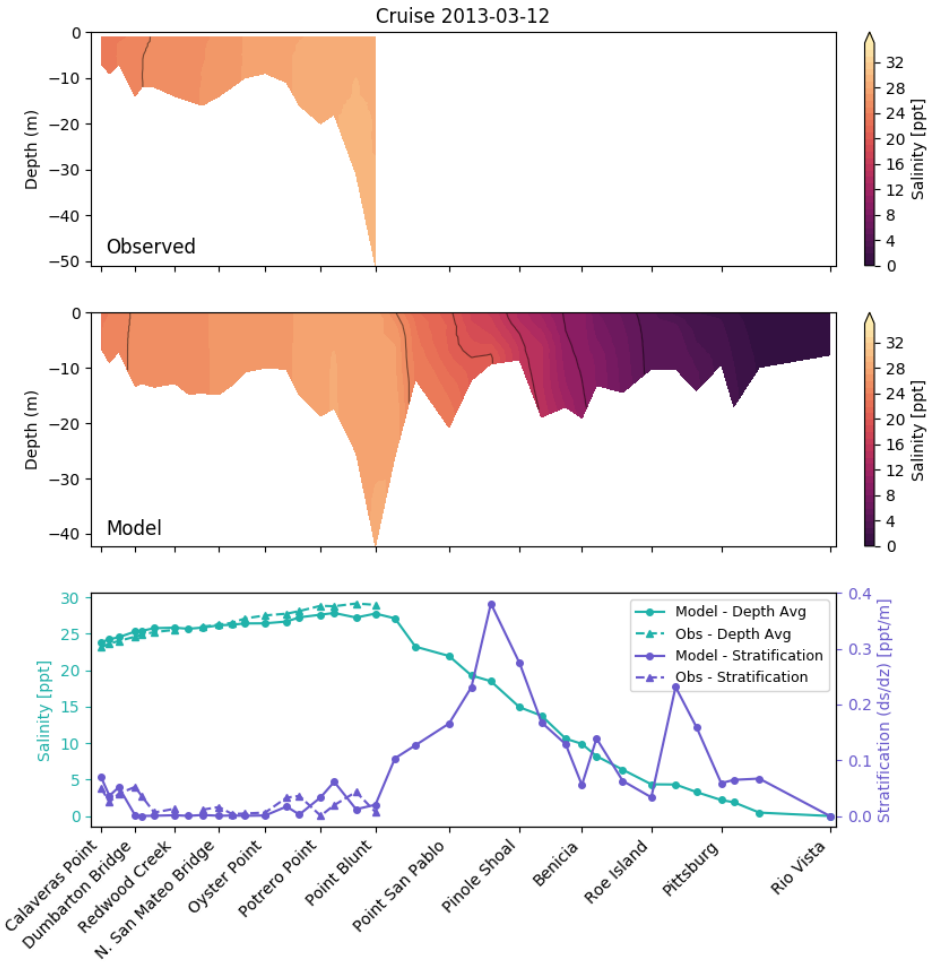

Figure 58: USGS Transect, 2013-03-12

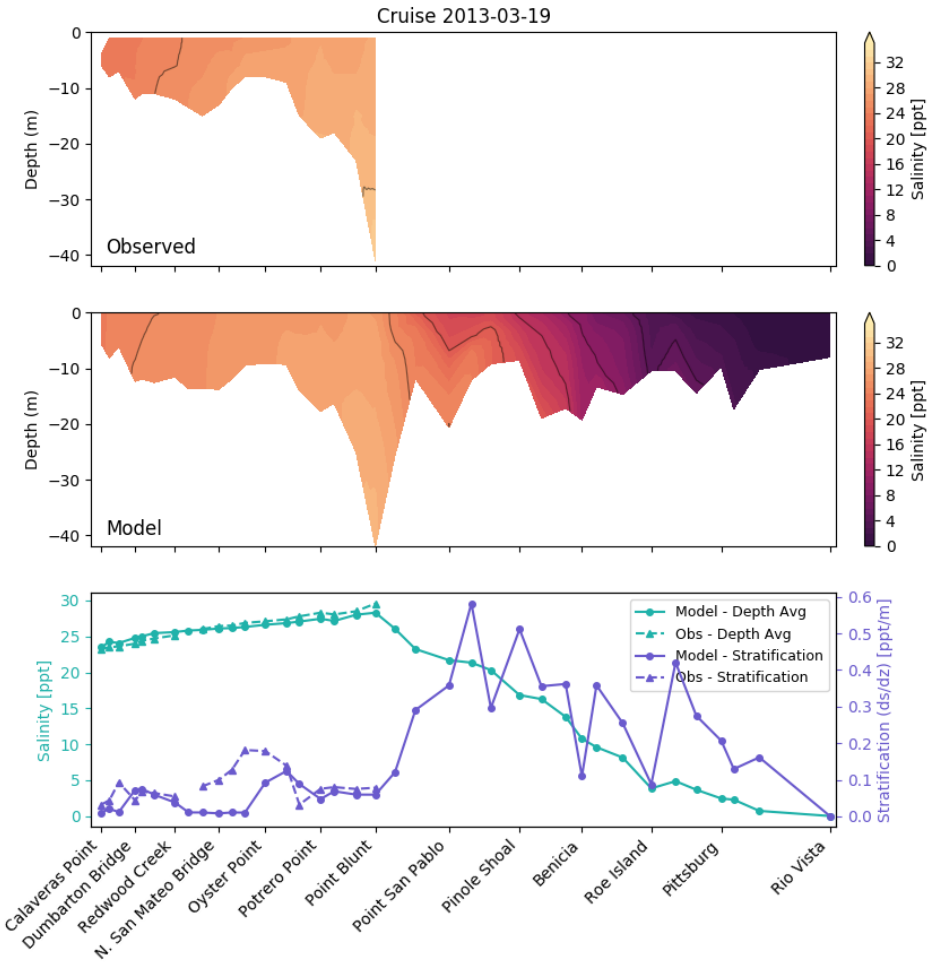

Figure 59: USGS Transect, 2013-03-19

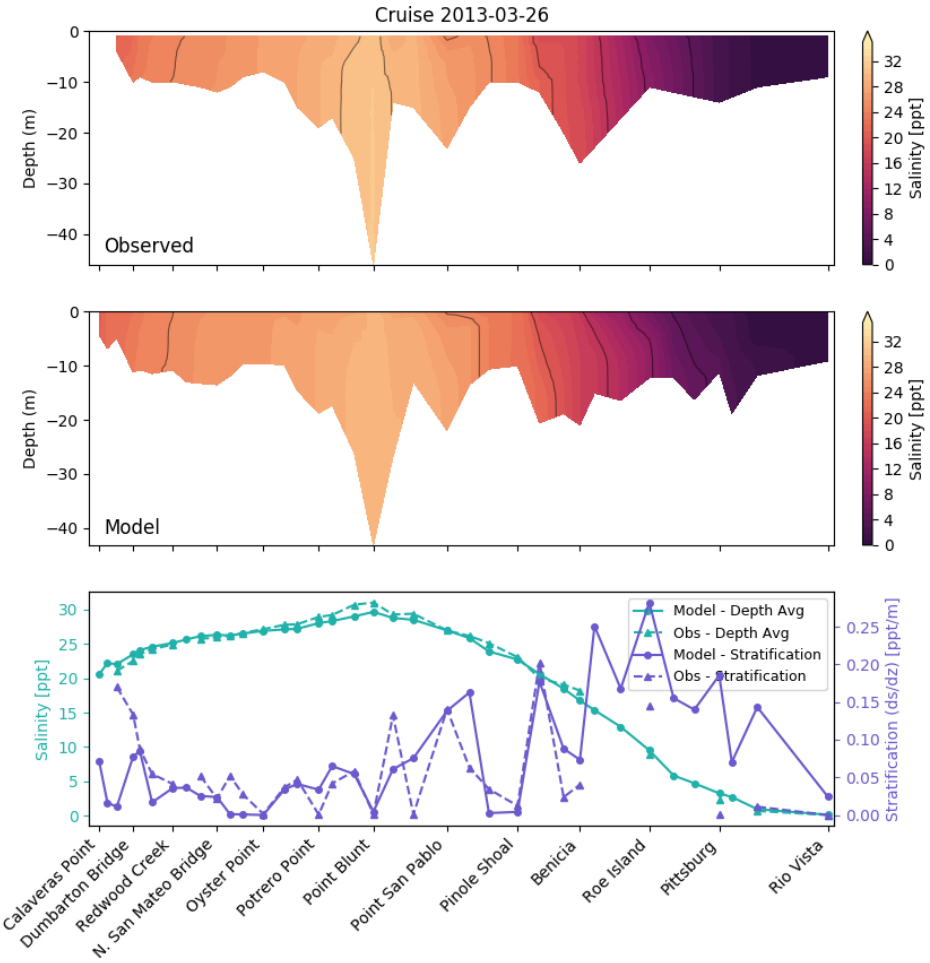

Figure 60: USGS Transect, 2013-03-26

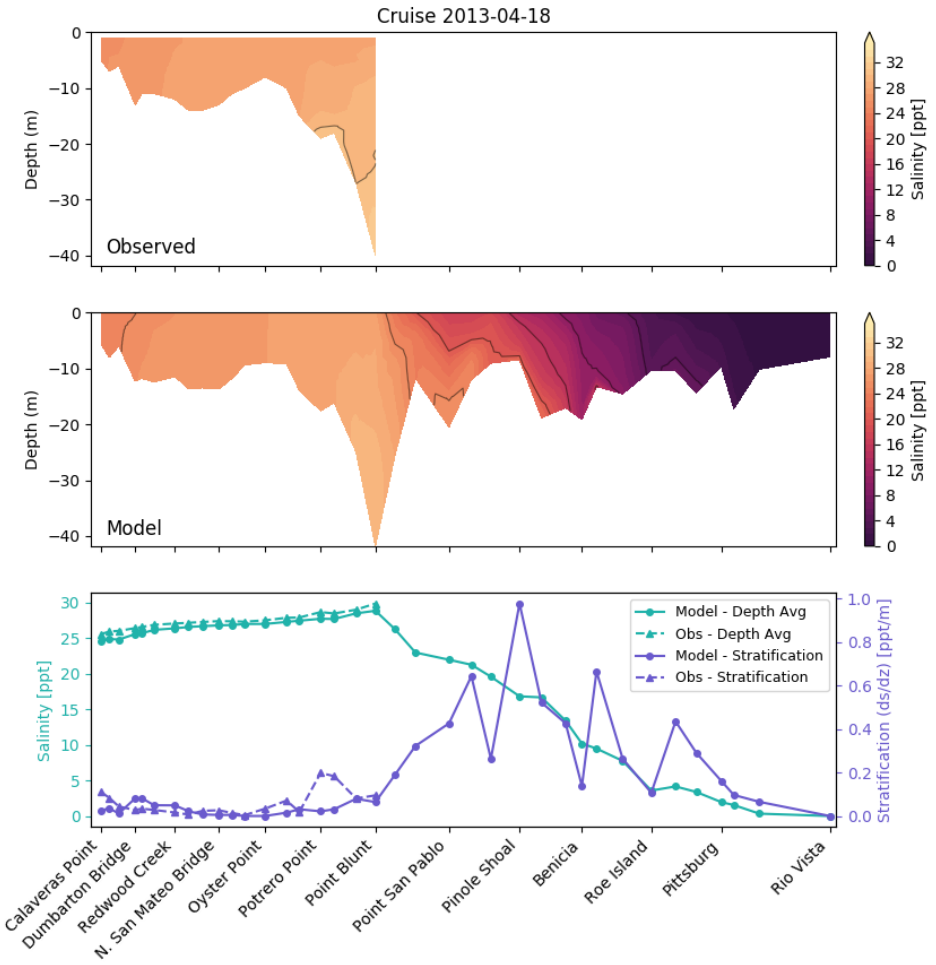

Figure 61: USGS Transect, 2013-04-18

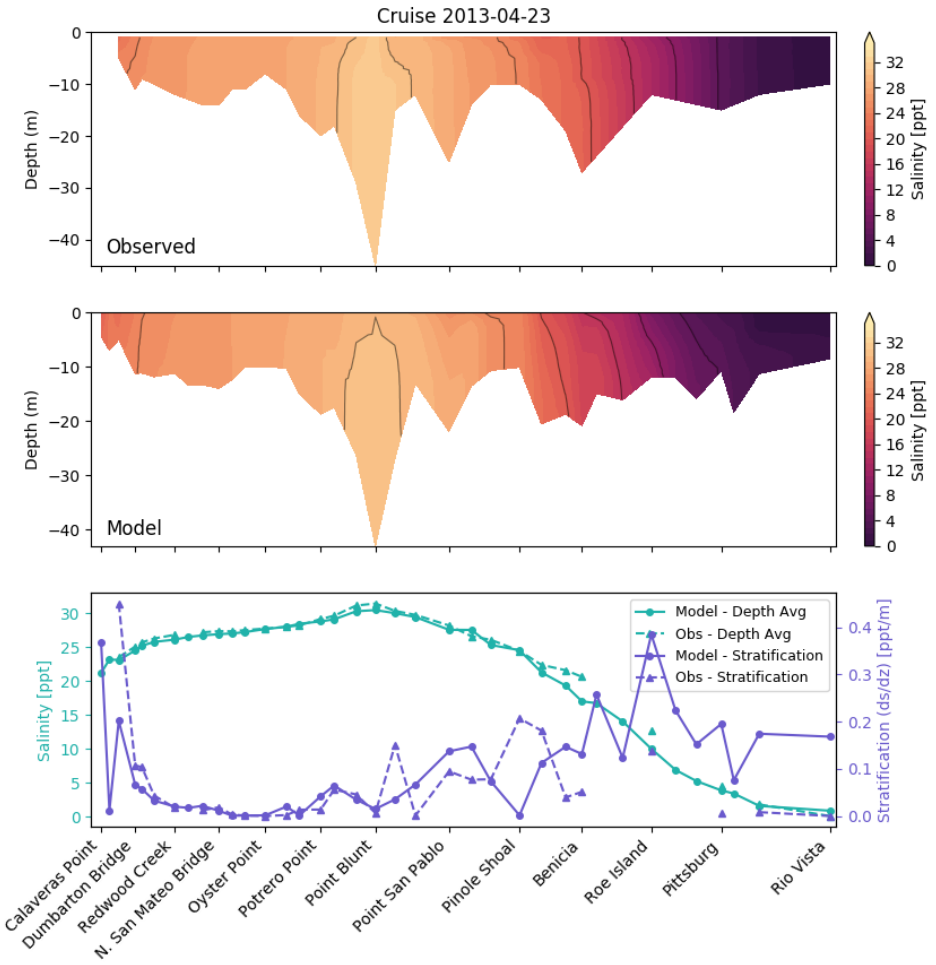

Figure 62: USGS Transect, 2013-04-23

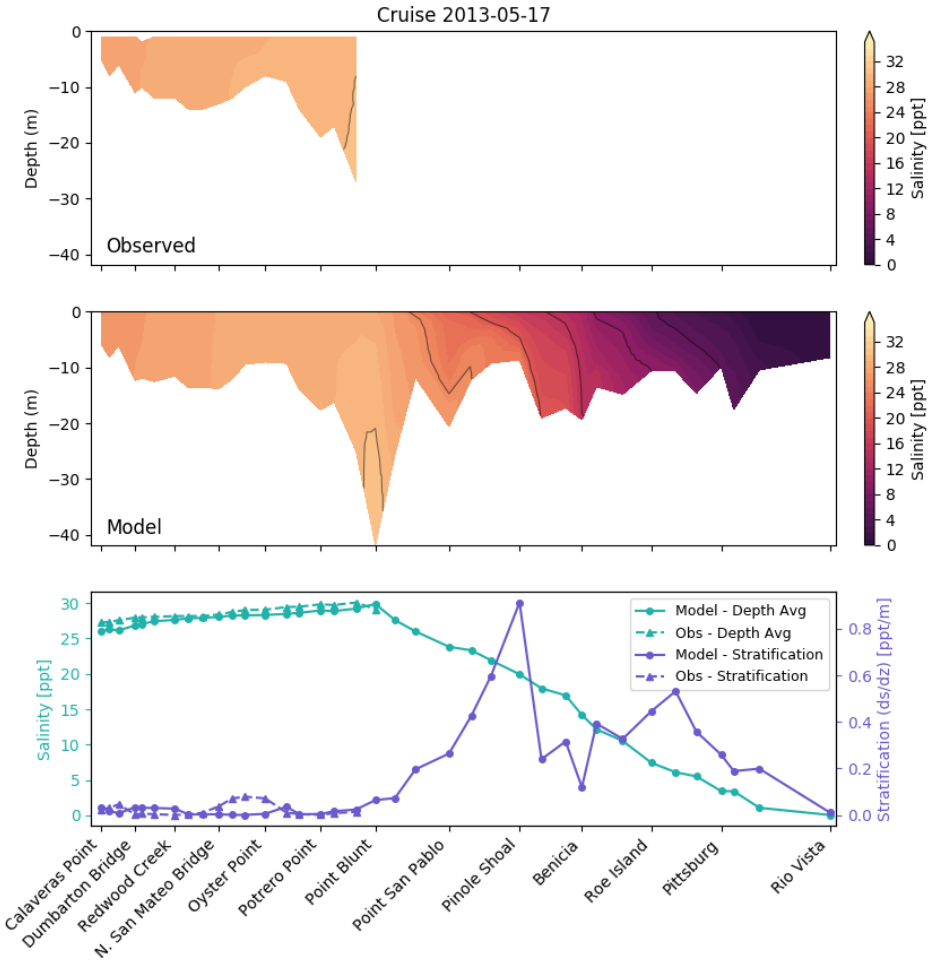

Figure 63: USGS Transect, 2013-05-17

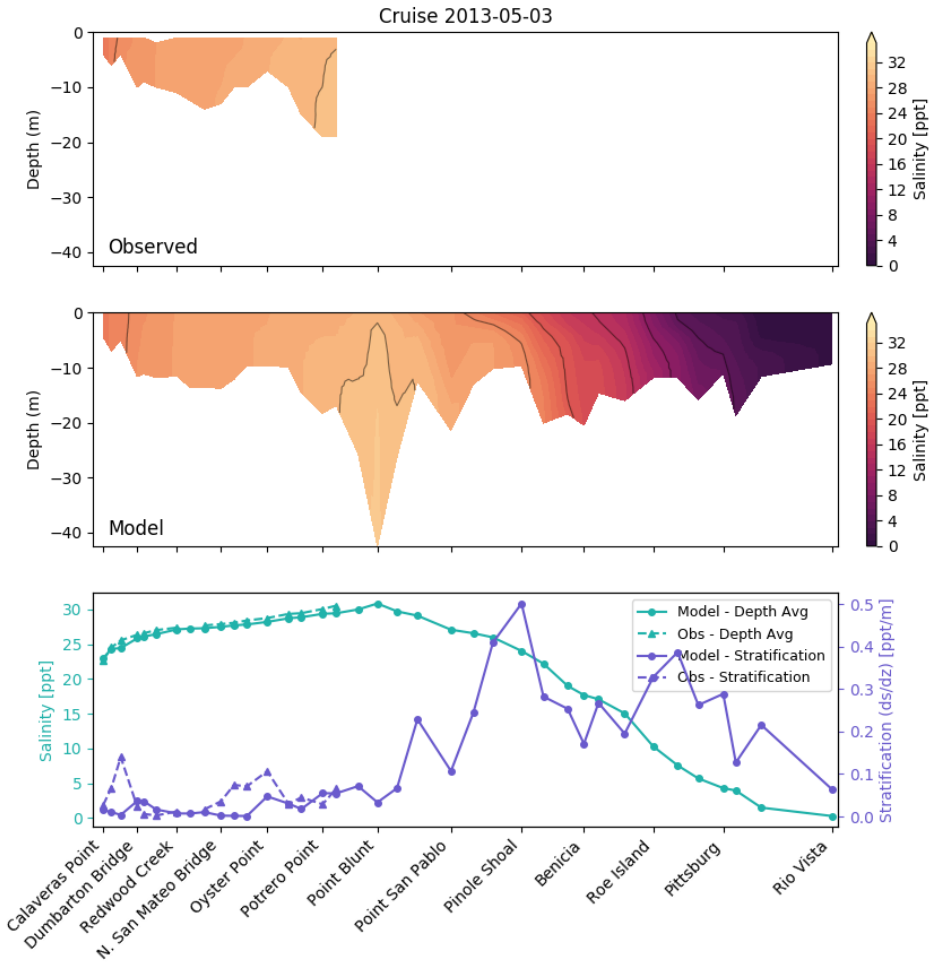

Figure 64: USGS Transect, 2013-05-03

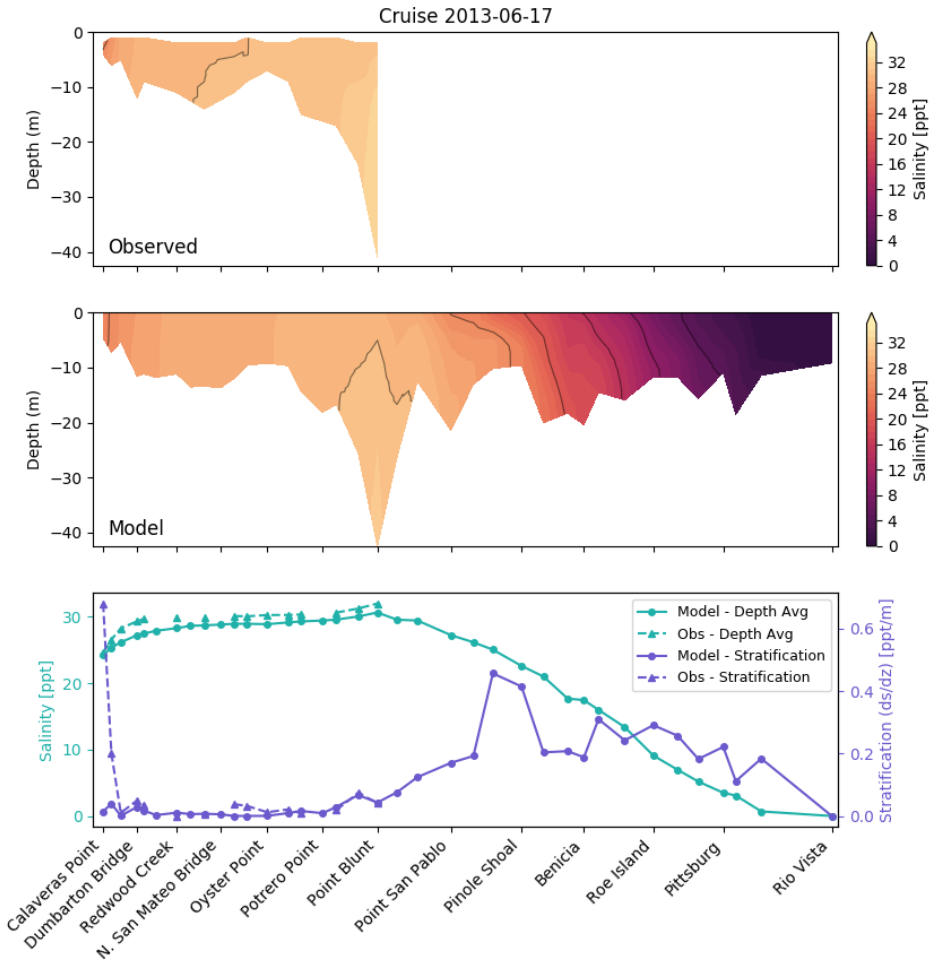

Figure 65: USGS Transect, 2013-06-17

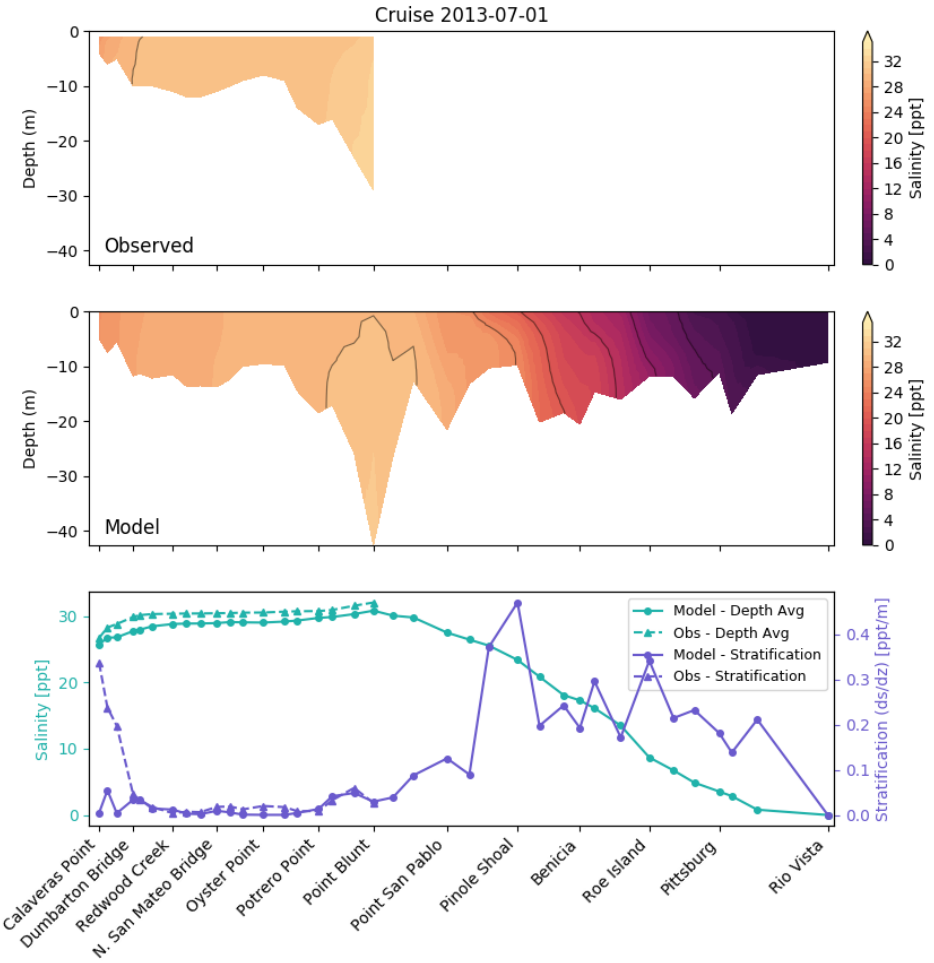

Figure 66: USGS Transect, 2013-07-01

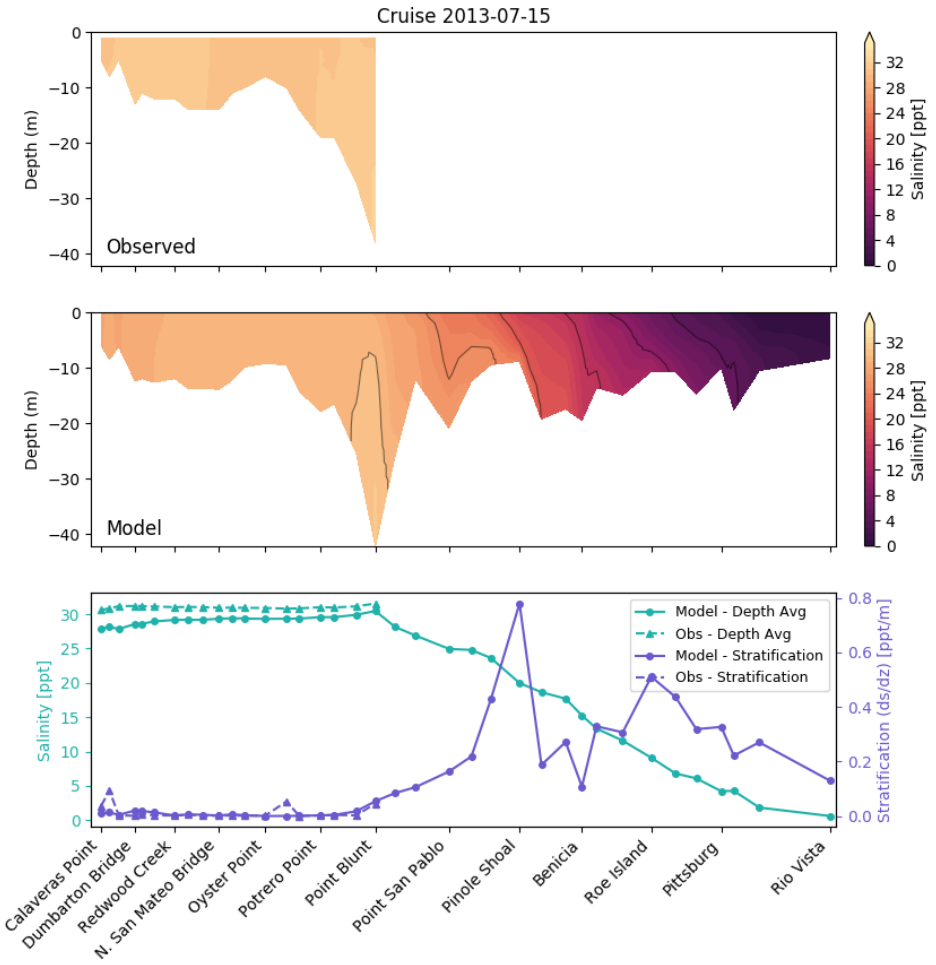

Figure 67: USGS Transect, 2013-07-15

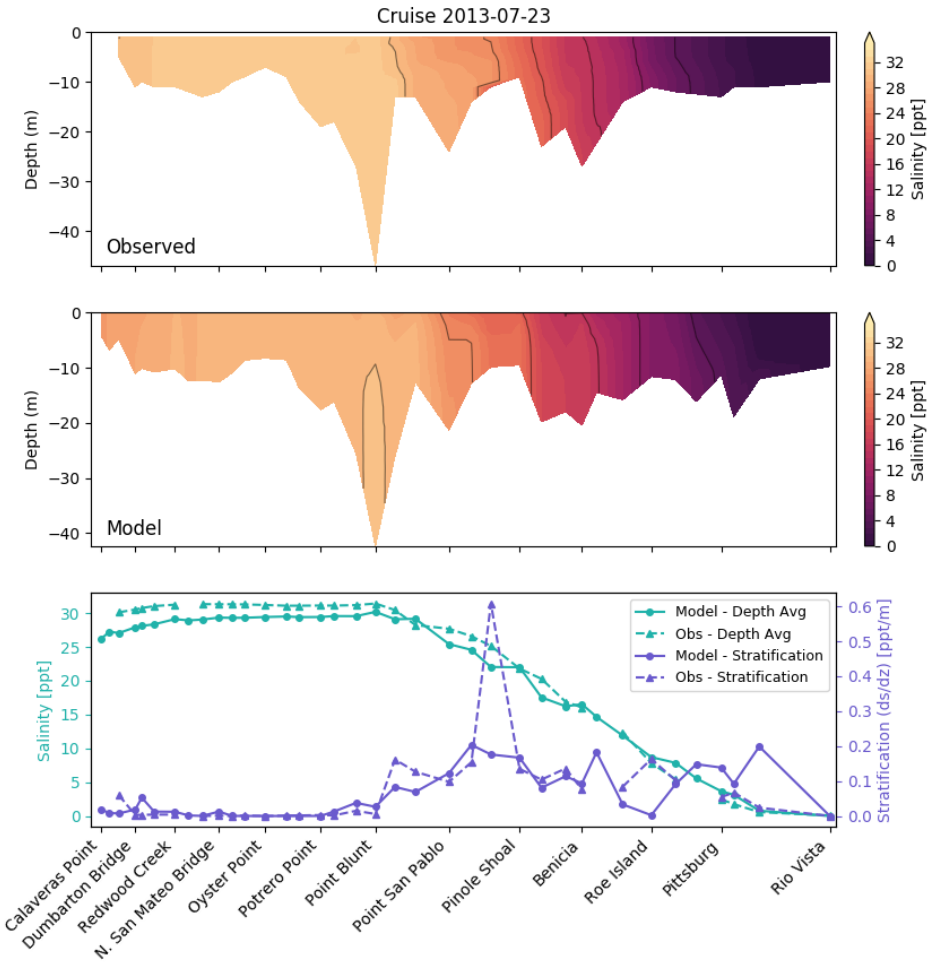

Figure 68: USGS Transect, 2013-07-23

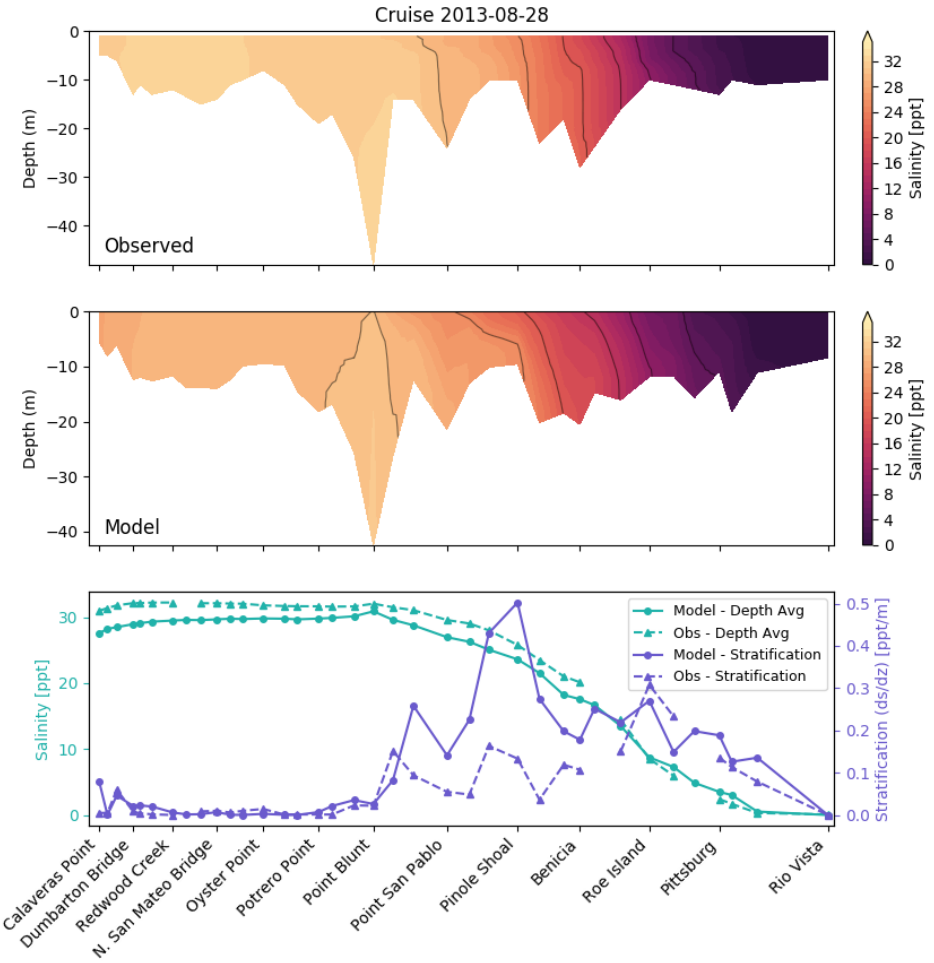

Figure 69: USGS Transect, 2013-08-28

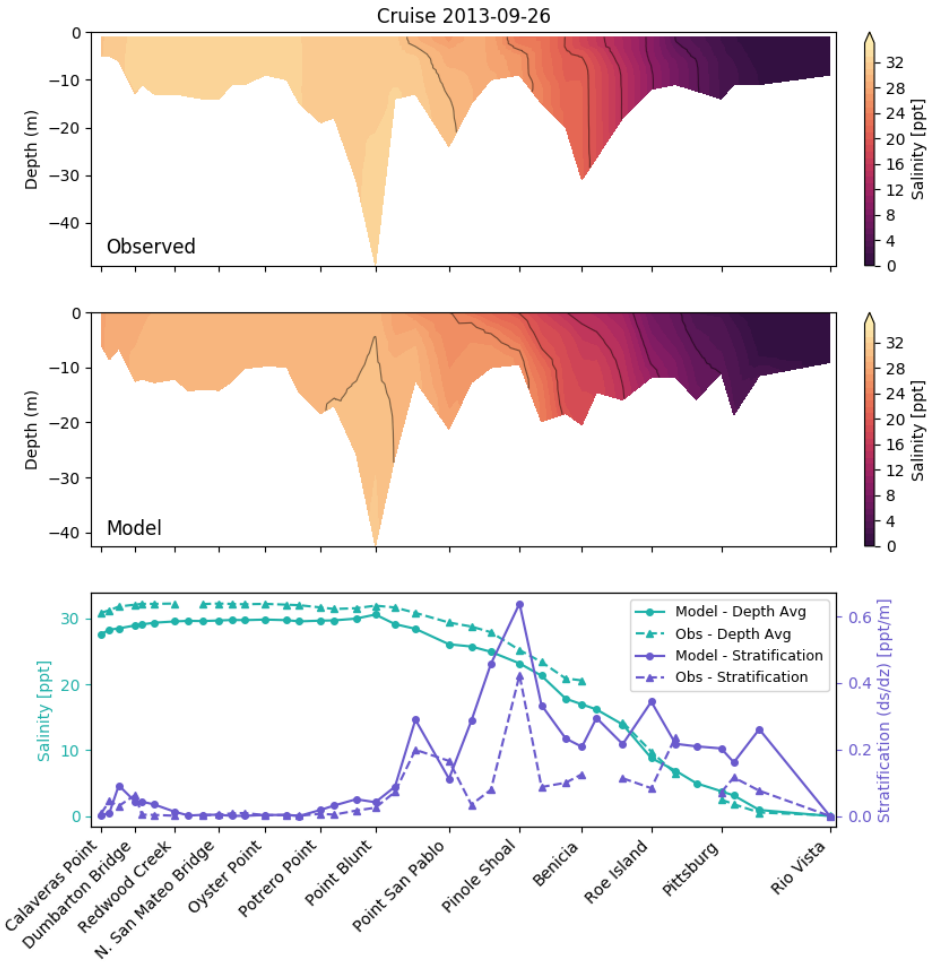

Figure 70: USGS Transect, 2013-09-26

5.4.2 Time Series

In addition to the transect data shown in the previous section, USGS maintains a limited number of mooring sites within the Bay. Four of these sites have salinity data overlapping the simulation period, and model-data comparisons for these are included below. While many of the large-scale patterns of salinity in the Bay can be extracted from the monthly transect data, high-frequency measurements allow for more rigorous skill metrics, and analysis of daily and spring-neap time scales.

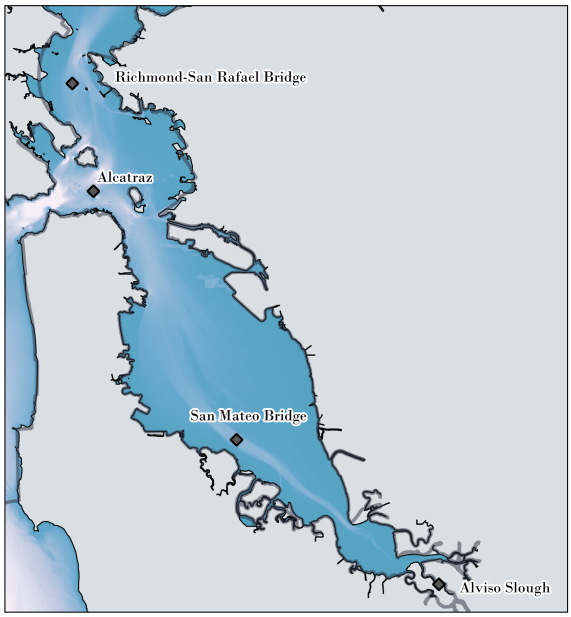

Figure 71: Location of USGS moorings used for salinity time series comparison.

Sites at the Richmond-San Rafael Bridge and the San Mateo Bridge consist of sensors at two fixed elevations. Alcatraz and Alviso each have a single sensor. Error metrics are calculated for the depth-averaged salinity. Skill and bias are reasonable for the open-Bay sites, with errors on the order of 2 ppt largely due to the previously mentioned bias low. Alviso Slough has been included for completeness, though its location in the margins is unlikely to validate well given the coarse representation of this region in the present model. A related modeling effort in the Nutrient Management Strategy is developing a hydrodynamic model focused on small scale features in Lower South Bay.

Name	Skill	Bias (ppt)	r^2	RMSE (ppt)
San Mateo Bridge	0.956	-0.50	0.972	1.06
Alcatraz	0.879	-0.88	0.925	1.43
Richmond Bridge	0.889	-1.53	0.924	1.89
Alviso Slough	0.556	8.88	0.598	10.35

Individual time series are shown below. For each site, salinity is extracted from the model at elevations matching the sensor(s) for that site. The upper panel in each of the figures below shows the average salinity (average of top and bottom sensors where available) with a 40 h low-pass filter (Hanning FIR). The shaded regions around the lines show the salinity range, as an approximation for tidal variability.

The lower figure shows an estimate of stratification. For sites with two sensors, stratification is calculated as the gradient between the two sensor elevations. For sites with a single sensor, stratification cannot be inferred from the observations, and the modeled stratification is extracted across the full water column.

Though the model output is not expected to validate well in the spinup period before Oct 1, 2012, these figures include that period to help evaluate the duration of the spinup period and potential drivers of dry-weather salinity bias.

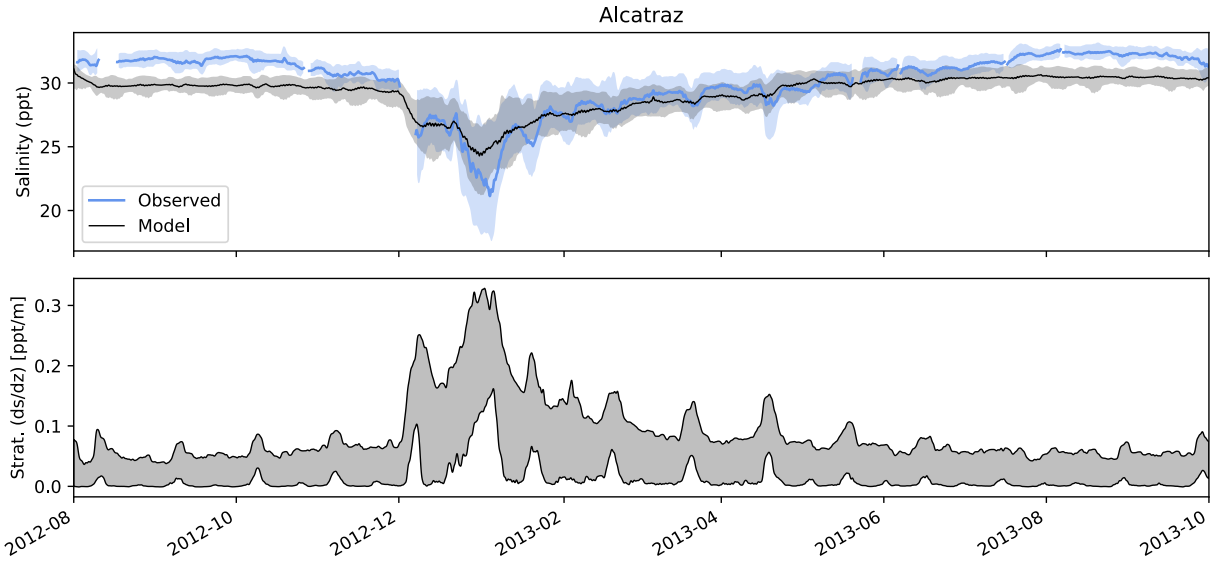

Figure 72: Salinity time series: Alcatraz, USGS 374938122251801

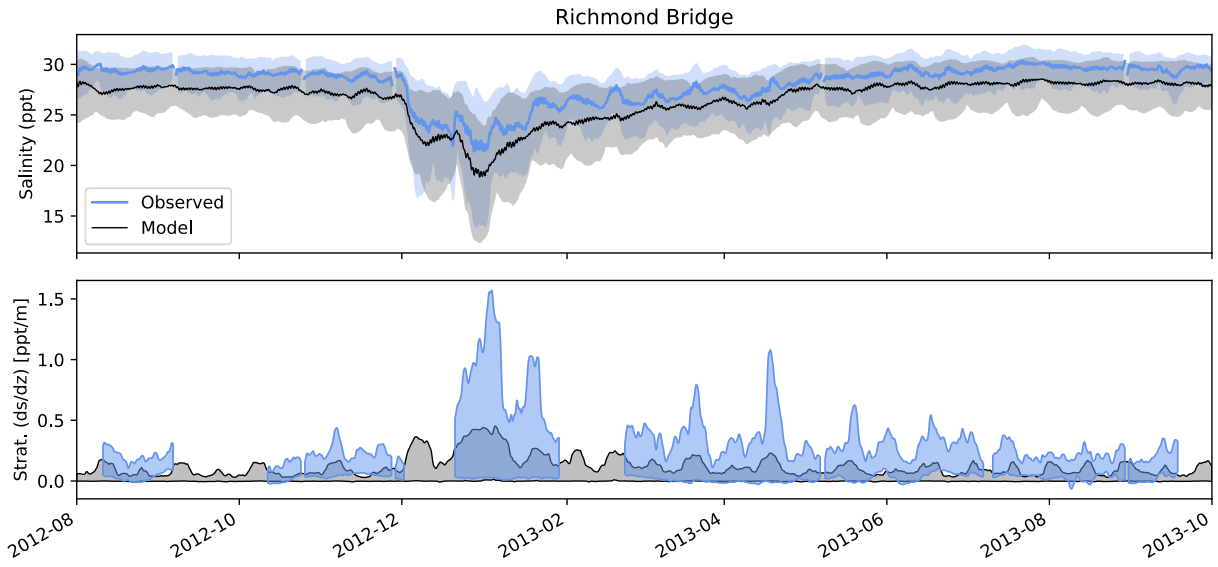

Figure 73: Salinity time series: Richmond / San Rafael Bridge, USGS 375607122264701

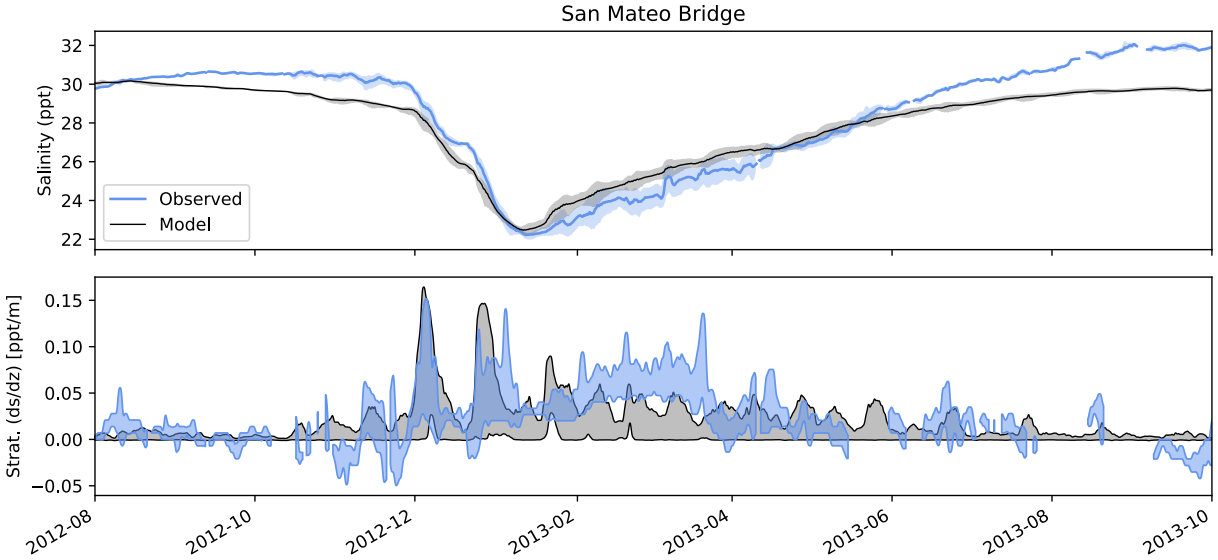

Figure 74: Salinity time series: San Mateo Bridge, USGS 11162765

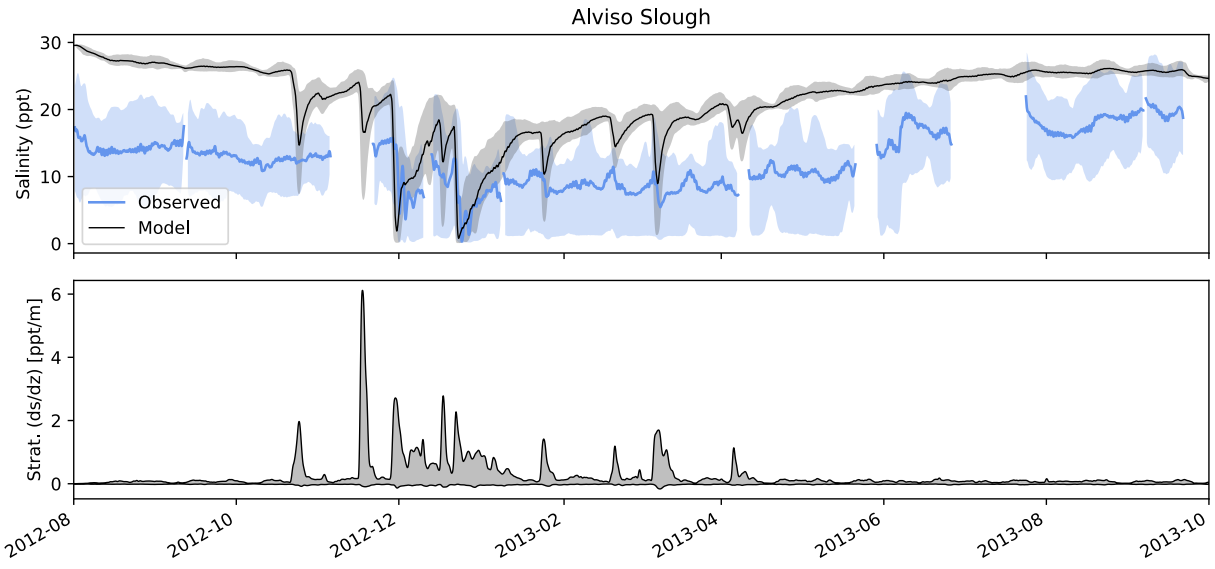

Figure 75: Salinity time series: Alviso Slough, USGS 11169750

6 Next Steps

The above model-data comparisons show that the model does well resolving the important transport processes in South Bay, and adequately resolves mixing and transport in Central Bay and San Pablo Bay. At the same time, the comparisons point to several potential improvements which will be tested and incorporated in the future.

Refine the forcing of the open ocean boundary The closed boundaries on the north and south sides of the coastal portion of the domain appear to decrease flushing of the San Francisco Bight, leading to too much retention of fresh water in Central Bay. We anticipate that allowing fluxes through these boundaries would improve salinity validation. Some experimentation is needed to determine the exact type of boundary condition to impose, as instabilities may arise when an open boundary is close to a high-gradient location like Point Reyes.

Delta Inflows Boundary conditions at the Delta currently come from a pair of high frequency velocity gaging stations. In the existing configuration these flows enter with zero salinity, but in particularly dry conditions flows here may have significant salinity. This discrepancy would lead to a non-physical loss of

salt. Forcing with time-varying salinity or imposing this boundary farther upstream would avoid this issue.

The Delta flows are also incomplete, and should be extended to include Dutch Slough and Threemile Slough. These channels carry much smaller fluxes than the Sacramento and San Joaquin Rivers, but given the importance of Delta flows overall, even these secondary inputs could be significant to downstream conditions.

The poor tidal phasing in the current model is also a point of potential improvement. This may be remedied to some extent by including the two additional flows mentioned above. To make more significant gains may require either a schematized Delta (e.g. a pair of dissipative channels mimicking the effects of the true Delta), or a Riemann boundary condition which would allow excess tidal energy to propagate out of the domain.

Evaporation Direct precipitation and evaporation are currently included in the model as time-varying but spatially constant quantities. Evaporation is under-represented due to stability issues in earlier iterations of the model. This factor will be relaxed in future runs, which we expect to cause an increase in modeled summer salinities in South Bay. Spatially-varying precipitation and evaporation would be more realistic, although this enhancement is not expected to make a large difference in the modeled salinities.

7 References

Foxgrover, A.C., Finlayson, D.P., Jaffe, B.E., and Fregoso, T.A., 2014, Bathymetry and Digital Elevation Models of Coyote Creek and Alviso Slough, South San Francisco Bay, California (ver. 3.0, September, 2015): U.S. Geological Survey Open-File Report 2011-1315, 20 p., https://dx.doi.org/10.3133/ofr20111315.

Ludwig, F. L., J. M. Livingston, and R. M. Endlich, 1991: Use of Mass Conservation and Dividing Streamline Concepts for Efficient Objective Analysis of Winds in Complex Terrain, J. Appl. Meteorol., Vol. 30, pp. 1490–1499.

Martyr-Koller, R.C., H.W.J. Kernkamp, A. van Dam, M. van der Wegen, L.V. Lucas, N. Knowles, B. Jaffe, T.A. Fregoso, Application of an unstructured 3D finite volume numerical model to flows and salinity dynamics in the San Francisco Bay-Delta, 2017. Estuarine, Coastal and Shelf Science, Vol. 192, pp 86–107, https://doi.org/10.1016/j.ecss.2017.04.024.

Pubben, S., 3D mixing patterns in San Francisco South Bay, 2017. Masters Thesis, TU Delft.

Vroom, J., van der Wegen, M., Martyr-Koller, R. C., and Lucas, L. V. (2017). What determines water temperature dynamics in the San Francisco Bay-Delta system? Water Resources Research, 53, https://doi.org/10.1002/2016WR020062

Wang, R. and Ateljevich, E. (2012). A Continuous Surface Elevation Map for Modeling (Chapter 6). In Methodology for Flow and Salinity Estimates in the Sacramento-San Joaquin Delta and Suisun Mars, 23rd Annual Progress Report to the State Water Resources Control Board. California Department of Water Resources, Bay-Delta Office, Delta Modeling Section.

Willmott, C.J., 1981: On the Validation of Models, J. Geophys. Res., Vol. 112, C01013.